

# A nonparametric Bayesian approach for simulation optimization with input uncertainty

Haowei Wang, Xun Zhang, Szu Hui Ng

Department of Industrial Systems Engineering and Management, National University of Singapore, SG 117576,  
haowei.wang@u.nus.edu, e0225088@u.nus.edu, isensh@nus.edu.sg

Stochastic simulation models are increasingly popular for analyzing complex stochastic systems. However, the input distributions required to drive the simulation are typically unknown in practice and are usually estimated from real world data. Since the amount of real world data tends to be limited, the resulting estimation of the input distribution will contain errors. This estimation error is commonly known as input uncertainty. In this paper, we consider the stochastic simulation optimization problem when input uncertainty is present and assume that both the input distribution family and the distribution parameters are unknown. We adopt a nonparametric Bayesian approach to model the input uncertainty and propose a nonparametric Bayesian risk optimization (NBRO) framework to study simulation optimization under input distribution uncertainty. We establish the consistency and asymptotic normality of the value of the objective function, the optimal solution, and the optimal value for the NBRO problem. We further propose a simulation optimization algorithm based on Efficient Global Optimization (EGO), which explicitly takes into account the input uncertainty so as to efficiently solve the NBRO problem. We study the consistency property of the modified EGO algorithm and empirically test its efficiency with an inventory example and a critical care facility problem.

*Key words:* Gaussian process, stochastic simulation optimization, input uncertainty, asymptotic properties, Efficient global optimization

---

## 1. Introduction

In many practical problems, one common task for the decision maker is to make decisions so as to optimize the performance of a system. In an inventory system, for example, a manager needs to decide the optimal ordering level. As real systems can be quite complex, directly conducting physical experiments on the real systems can be extremely expensive. To cope with this, simulation models are increasingly being used by practitioners to make inferences about the system and to make decisions. These simulation models are approximations of the real systems, and are typically cheaper and easier to develop. Such an optimization via

simulation (OvS) approach, also referred to as simulation optimization, aims to find the best design variable that optimizes some simulation output values. One classical stochastic simulation optimization problem (minimization) is formulated as

$$\min_{\mathbf{x} \in \mathcal{X}} \mathbb{E}_{\boldsymbol{\xi} \sim P^c} [h(\mathbf{x}, \boldsymbol{\xi})] \quad (1)$$

where  $\mathbf{x} \in \mathbb{R}^d$  is the design variable that we aim to minimize with a continuous box-constraint design space  $\mathcal{X}$ ,  $\boldsymbol{\xi} \in \mathbb{R}^l$  is a random variable that accounts for the random effects of the system,  $h$  is the simulation output that depends on both  $\mathbf{x}$  and  $\boldsymbol{\xi}$ , which is stochastic due to the randomness of  $\boldsymbol{\xi}$ , e.g., the  $h(\mathbf{x}, \boldsymbol{\xi})$  can be the simulated steady-state cost in the inventory problem, which is stochastic as it depends on the random demand  $\boldsymbol{\xi}$ . The expectation in (1) is taken with respect to the distribution of  $\boldsymbol{\xi}$ , i.e.,  $\boldsymbol{\xi} \sim P^c$ . This  $P^c$  is usually referred to as the true input distribution (Zhou and Xie 2015, Wu et al. 2018).

In practice, however, the true input distribution that drives the simulation run is usually unknown. Only a finite set of real world data  $\boldsymbol{\xi}_1, \dots, \boldsymbol{\xi}_n \sim P^c$  is available, from which an estimated input distribution, denote by  $\hat{P}$  can be obtained. One common approach is to treat  $\hat{P}$  as the true input distribution and the uncertainty arising from the estimation is ignored. Then the following problem is usually considered instead:

$$\min_{\mathbf{x} \in \mathcal{X}} \mathbb{E}_{\boldsymbol{\xi} \sim \hat{P}} [h(\mathbf{x}, \boldsymbol{\xi})] \quad (2)$$

If the size  $n$  of the dataset is small, this may lead to a poor estimation  $\hat{P}$ . Then the best design for solving problem (2) can be quite different from that of (1), and hence the obtained design can be sub-optimal or even wrong. The uncertainty arising from a finite data estimation is called input uncertainty, and ignoring the input uncertainty can have a nonnegligible impact on the evaluation of the performance of the system (Song et al. 2014, Lam 2016) as well as on the simulation optimization (Wu et al. 2018, Wang et al. 2019a).

There has been quite a sizeable literature focusing on solving the stochastic simulation optimization problem given by (2), ignoring input uncertainty. There are three main streams in this literature: methods involving metaheuristics (Ólafsson 2006), gradient based methods (Kushner and Yin 2003), and metamodel based methods (Barton and Meckesheimer 2006). These three types of methods have been shown to be efficient at solving (2), and each has its own advantages and limitations, under different scenarios. Metamodels, the statistical approximate models of the simulation models, are easy to

develop. Besides, metamodel-based methods require no strict assumptions on the objective functions, making them more attractive in pragmatic applications. [Xu et al. \(2015\)](#) provides a comprehensive review of simulation optimization methods.

Although most simulation optimization methods can only be applied directly to the case when the input uncertainty is ignored, some recent research has started trying to take input uncertainty into account in the simulation optimization problem. Realizing the risk in solving problem (2), [Zhou and Xie \(2015\)](#) considered a simplified case where the input distribution belongs to a known parametric family and  $\mathbf{P}^c$  can be fully characterized by an unknown input parameter  $\boldsymbol{\lambda}^c$ , i.e.,  $\mathbf{P}^c = \mathbf{P}_{\boldsymbol{\lambda}^c}$ . They tried to find how to consider the input uncertainty arising from not exactly knowing  $\boldsymbol{\lambda}^c$  in simulation optimization. By taking a Bayesian perspective, [Zhou and Xie \(2015\)](#) viewed  $\boldsymbol{\lambda}^c$  as a random variable  $\boldsymbol{\lambda}$ . A prior was posed on  $\boldsymbol{\lambda}$  and a posterior distribution  $\boldsymbol{\pi}$  for  $\boldsymbol{\lambda}$  was then computed, conditionally on the real world data. This  $\boldsymbol{\pi}$  was then used to quantify the knowledge about the true input parameter  $\boldsymbol{\lambda}^c$ . Based on the posterior distribution, [Zhou and Xie \(2015\)](#) proposed the Bayesian Risk Optimization (BRO) framework:

$$\min_{\mathbf{x} \in \mathcal{X}} \rho_{\boldsymbol{\lambda} \sim \boldsymbol{\pi}} [\mathbb{E}_{\boldsymbol{\xi} \sim \mathbf{P}_{\boldsymbol{\lambda}}} [h(\mathbf{x}, \boldsymbol{\xi})]] \quad (3)$$

where  $\rho$  is a risk function which can be, for example, the expectation, the mean-variance, the value-at-risk (VaR), or the conditional value at risk (CVaR). [Zhou and Xie \(2015\)](#) pointed out that BRO outperforms (2) when the size  $n$  of the real world dataset is small and  $h$  is sensitive to  $\boldsymbol{\lambda}$ . [Wu et al. \(2018\)](#) further proved the consistency and asymptotic normality of the optimal value of the BRO for the four risk functions. [Pearce and Branke \(2017\)](#) and [Wang et al. \(2019a\)](#) proposed algorithms based on Gaussian processes to solve the BRO problem for the expectation risk function. However, all of these papers only consider the case that  $\boldsymbol{\xi}$  follows a distribution belonging to a known family. Taking the inventory problem as an example, a random demand  $\boldsymbol{\xi}$  is assumed to follow some parametric distribution, e.g.,  $\mathbf{P}^c = \exp(\boldsymbol{\lambda}_c)$ , where  $\boldsymbol{\lambda}_c$  is the unknown true input parameter. However, the assumption of a known family of distribution can be too restrictive in practice, especially for situations where no prior knowledge about the input distribution is available. In addition, real world data usually exhibit rich properties such as multi-modality, skewness, and excess kurtosis, which can not be captured well by the standard parametric families. Thus, there will always be a selection error for the distribution family, even when there

is a large amount of real world data. To mitigate the input distribution selection error, [Chick \(2001\)](#) proposed Bayesian Model Averaging (BMA), which takes into account both the uncertainty in the distribution family and in the input parameters. However, it can still be difficult to select several candidate parametric families in the first place.

Given the limitations of parametric approaches, modeling input uncertainty in a nonparametric perspective has been studied over the years ([Lam 2016](#)) in the stochastic simulation community. Existing methods, including direct resampling ([Barton and Schruben 1993](#)), bootstrap resampling, uniformly randomized empirical distribution function ([Barton and Schruben 2001](#)), and Dirichlet process mixtures ([Xie et al. 2019](#)), aim to quantify the input uncertainty and construct confidence intervals of the simulation output ([Ankenman and Nelson 2012](#), [Song and Nelson 2015](#)). However, none of them considers the impact of this uncertainty on the simulation optimization. To the best of our knowledge, the inclusion of input uncertainty in the stochastic simulation optimization problem when neither the input distribution family nor the input parameter is known has not yet been comprehensively explored. In the present paper, we consider the stochastic simulation optimization problem when the distribution family of  $\mathbf{P}^c$  is unknown. In addition, we focus on the risk neutral case and choose the expectation risk function. Specifically, we first extend the BRO problem with the expectation risk function to the case when the distribution family of  $\mathbf{P}^c$  is unknown, and we call this the extended Nonparametric Bayesian Risk Optimization (NBRO) problem. We further provide the asymptotic properties of the NBRO problem. Then we modify a metamodel-based method, the popular Efficient Global Optimization (EGO) algorithm, to solve the NBRO problem. We provide both the theoretical and empirical convergence for our proposed algorithm to illustrate its efficiency. The proposed algorithm can be viewed as an extension of [Wang et al. \(2019a\)](#), whose algorithms can only be applied when the input distribution family is known.

The rest of this paper is organized as follows. Section 2 introduces a nonparametric Bayesian modeling approach to the input distribution and formulates the NBRO problem. Section 3 provides the consistency and asymptotic normality properties of the value of the objective function, optimal solution, and optimal value obtained from the NBRO problem. The modified EGO algorithm for solving the NBRO as well as its theoretical convergence properties are introduced in Section 4. In Section 5, we present the results of experiments involving an inventory example and a critical care facility problem to show the empirical

convergence of our proposed algorithm, as well as the advantages of the NBRO which considers input uncertainty over an approach ignoring input uncertainty. The whole article is concluded in Section 6 and future directions are discussed.

## 2. The nonparametric Bayesian risk optimization (NBRO) problem

In this section, we will extend the BRO problem (given by (3)) to the case when the input distribution family of  $P^c$  is unknown. We will refer to the extended problem as the Nonparametric Bayesian Risk Optimization (NBRO) problem.

### 2.1. Bayesian Risk Optimization (BRO) with expectation risk function

In order to hedge the risk of solving the approximate problem given by (2), instead of using the estimator  $\hat{P}$ , we model  $P^c$  with a posterior  $P \sim \pi$  and aim to solve the following problem:

$$\min_{\mathbf{x} \in \mathcal{X}} g(\mathbf{x}) = E_{P \sim \pi} [E_{\xi \sim P} [h(\mathbf{x}, \xi)]] . \quad (4)$$

The outer expectation in (4) is taken with respect to the posterior of  $P$ . The inner expectation is taken with respect to the distribution of  $\xi$ . The original BRO problem proposed by Zhou and Xie (2015) assumed the distribution family for  $P$  to be known and that the distribution can be characterized by the input parameter  $\lambda$ . Then the formulation given by (4) can be reduced to Equation (3). Here, we aim to extend the BRO problem to consider a more general case in which the distribution family is unknown, and the input distribution  $P$  is modeled with a nonparametric Bayesian approach.

### 2.2. Nonparametric Bayesian modeling of the input distribution and nonparametric Bayesian risk optimization (NBRO)

In the following, we introduce a nonparametric Bayesian approach to modeling the unknown input distribution.

Recall  $P^c$  is the true input distribution from which the real world data are collected. Denote the real world data set by  $D_n = \{\xi_1, \dots, \xi_n\}$ . From the frequentist perspective, the empirical distribution function  $\hat{P}$  can be used to estimate  $P^c$  as follows:  $\hat{P}(t) = \frac{1}{n} \sum_{i=1}^n I(\xi_i \leq t)$ . An alternative way to estimate  $P^c$  is from a Bayesian perspective, where we model the unknown  $P^c$  as a random  $P$ . Specifically, a prior  $\pi_0(P)$  is first assumed on  $P$ , which is our initial belief about  $P^c$ . Then, given the real world data  $D_n$ , the posterior

distribution of  $\mathbf{P}$  is updated as  $\pi(\mathbf{P}|\mathbf{D}_n)$  which is our current knowledge of  $\mathbf{P}^c$  after observing  $\mathbf{D}_n$ . One advantage of the Bayesian approach over the frequentist approach is that we can incorporate prior knowledge about the real input process in the prior distributions. If no prior knowledge is available or assumed, non-informative priors can be used. In this paper, we assume that no information about the input distribution family is available. In this case, the parametric Bayesian approach to model the input uncertainty (Wang et al. 2019a) can not be used. The most commonly used prior for distributions without the assumption of a parametric family is the conjugate Dirichlet process prior (Ferguson 1973).

The Dirichlet process is a family of stochastic processes whose realizations are probability distributions. The Dirichlet process prior can be parametrized by the concentration parameter  $\alpha$  and the base distribution  $\mathbf{P}_0$ , and is then denoted by  $DP(\alpha, \mathbf{P}_0)$ . The base distribution  $\mathbf{P}_0$  is a distribution that can be thought of as a prior guess for  $\mathbf{P}^c$ . It is the mean value of the Dirichlet process, which draws distributions “around” it. The parameter  $\alpha$  controls how tightly concentrated the prior is around  $\mathbf{P}_0$ . The larger the concentration parameter, the more concentrated the prior is around  $\mathbf{P}_0$ . Therefore, high values of  $\alpha$  imply high confidence in  $\mathbf{P}_0$  and a low  $\alpha$  represents a vague belief. The concentration parameter  $\alpha$  can be thought of as the number of “initial” data points to obtain  $\mathbf{P}_0$ . Given the real world data  $\xi_1, \dots, \xi_n \sim \mathbf{P}^c$  and the chosen Dirichlet process  $DP(\alpha, \mathbf{P}_0)$  as the prior, we can derive the posterior distribution, which is also a Dirichlet process:

$$\pi(\mathbf{P}|\xi_1, \dots, \xi_n) \sim DP\left(\alpha + n, \frac{\alpha\mathbf{P}_0 + \sum_{j=1}^n \delta_{\xi_j}}{\alpha + n}\right).$$

where  $\delta$  is the Dirac delta measure

$$\delta_{\xi_i}(E) = \begin{cases} 1 & \text{if } \xi_i \in E \\ 0 & \text{if } \xi_i \notin E \end{cases} \quad (5)$$

where  $E$  is any event in the event space. The base distribution, which is the mean of the posterior Dirichlet process as well, becomes  $\frac{\alpha\mathbf{P}_0 + \sum_{j=1}^n \delta_{\xi_j}}{\alpha + n} = \frac{\alpha}{\alpha + n}\mathbf{P}_0 + \frac{n}{\alpha + n}\left(\frac{1}{n}\sum_{j=1}^n \delta_{\xi_j}\right)$ , which is a weighted average of the prior base distribution  $\mathbf{P}_0$  and the empirical distribution  $\frac{1}{n}\sum_{j=1}^n \delta_{\xi_j}$ . With  $P \sim \pi(P|\xi_1, \dots, \xi_n)$ , our knowledge about  $\mathbf{P}^c$  as well as the corresponding input uncertainty can be quantified. As  $n$  goes to infinity, the posterior Dirichlet process will converge in distribution to the true input distribution  $\mathbf{P}^c$  (Hjort et al. 2010).

It is worth mentioning that Xie et al. (2019) adopted another nonparameteric Bayesian model, the Dirichlet Process Mixture model (DPM) to model the input uncertainty. The DPM uses component densities from a parametric family, such as gamma, normal, log-normal etc. and represents the weights of the mixture components with a Dirichlet Process. Here, we adopt the Dirichlet Process instead of the DPM for several reasons. The Dirichlet Process is flexible and has been successfully applied to capture different characteristics of distributions for different applications (Christensen and Johnson 1988, Heath et al. 2012, Barcella et al. 2018). It requires fewer assumptions than the DPM, for which appropriate parametric family needs to be carefully chosen based on empirical experience (Hjort et al. 2010). In addition, the posterior distribution of a Dirichlet Process prior is also a Dirichlet Process, and it is easy and cheap to obtain samples from the Dirichlet Process posterior using the algorithm of stick breaking process (Hjort et al. 2010). In contrast, the posterior of a DPM prior is intractable, and time-consuming Gibbs samplers are required to generate samples from the posterior. Furthermore, the present work focuses on the simulation optimization of expensive simulation models with a limited budget of simulation runs. In this situation, metamodels are needed to propagate the input uncertainty to the output and computational efficiency in constructing the models is required.

As we do not make any parametric assumptions on  $\mathbf{P}$ , we call problem (4) the Nonparametric Bayesian Risk Optimization (NBRO) problem, where the input distribution  $\mathbf{P}$  is modeled with the nonparameteric Bayesian approach described above.

### 3. Asymptotic properties of NBRO

In this section, we study the consistency and asymptotic normality of the NBRO problem. For consistency, we show that as the size  $n$  of the real world dataset tends to infinity: 1) the objective function of the NBRO, i.e.,  $\mathbb{E}_{\mathbf{P} \sim \pi}[\mathbb{E}_{\xi \sim \mathbf{P}}[h(\mathbf{x}, \xi)]]$ , will converge (in probability) pointwisely to true objective function  $\mathbb{E}_{\xi \sim \mathbf{P}^c}[h(\mathbf{x}, \xi)]$ ; 2) the optimal design (solution) obtained from NBRO,  $\mathbf{x}_n = \arg \min_{\mathbf{x}} \mathbb{E}_{\mathbf{P} \sim \pi}[\mathbb{E}_{\xi \sim \mathbf{P}}[h(\mathbf{x}, \xi)]]$ , will converge to the true optimal design:  $\mathbf{x}^* = \arg \min_{\mathbf{x}} \mathbb{E}_{\xi \sim \mathbf{P}^c}[h(\mathbf{x}, \xi)]$  in probability; 3) the optimal value,  $\mathbb{E}_{\mathbf{P} \sim \pi}[\mathbb{E}_{\xi \sim \mathbf{P}}[h(\mathbf{x}_n, \xi)]]$ , of the objective function of the NBRO will converge to the true optimal value  $\mathbb{E}_{\xi \sim \mathbf{P}^c}[h(\mathbf{x}^*, \xi)]$  of the objective function in probability. These consistency results support the method of solving the NBRO problem in (4), as it will approach the solution of the true problem in (1) as  $n$  gets large, even if the true underlying input distribution

$P^c$  is unknown. In the ideal case of an infinitely large sample size of the real observations, solving the NBRO problem is asymptotically equivalent to solving the true problem.

We also investigate the asymptotic normality property of the solutions as well as the function value. These results can provide confidence intervals for the value of the objective function, the optimal solution, and the optimal value. The confidence intervals can further be used to quantify the uncertainty in using the proposed NBRO framework. For example, one can specify a tolerance level of the variance (or the width of the confidence interval), based on which they can determine the minimum amount of real world data needed to achieve the target variance with the estimators of the asymptotic variances.

Both consistency and asymptotic normality are theoretical evidence supporting the assertion that NBRO is a well founded way to optimize the simulation system when the input uncertainty is modeled using the Dirichlet process. Before proceeding to the specific theorems and proofs, we make the following assumption about  $h(\mathbf{x}, \boldsymbol{\xi})$  and  $\boldsymbol{\xi}$ .

ASSUMPTION 1.

(i)  $h(\mathbf{x}, \boldsymbol{\xi})$  is Lipschitz in  $\mathbf{x}$  and  $\boldsymbol{\xi}$ , i.e., there exists positive constants  $L_1$ ,  $L_2$ , and  $L_3$  such that

$$|h(\mathbf{x}, \boldsymbol{\xi}_1) - h(\mathbf{x}, \boldsymbol{\xi}_2)| \leq L_1 \|\boldsymbol{\xi}_1 - \boldsymbol{\xi}_2\|, \quad \forall \mathbf{x}$$

$$|h(\mathbf{x}_1, \boldsymbol{\xi}) - h(\mathbf{x}_2, \boldsymbol{\xi})| \leq L_2 \|\mathbf{x}_1 - \mathbf{x}_2\|, \quad \forall \boldsymbol{\xi}.$$

$$\|\partial_{\mathbf{x}} h(\mathbf{x}_1, \boldsymbol{\xi}) - \partial_{\mathbf{x}} h(\mathbf{x}_2, \boldsymbol{\xi})\| \leq L_3 \|\mathbf{x}_1 - \mathbf{x}_2\|, \quad \forall \boldsymbol{\xi}.$$

where  $\partial_{\mathbf{x}}$  means taking the partial derivative with respect to  $\mathbf{x}$  and  $\|\cdot\|$  denotes the euclidean norm.

(ii)  $\boldsymbol{\xi}$  has bounded support, i.e., there exists a compact set  $\Omega = [\underline{\xi}_1, \bar{\xi}_1] \times [\underline{\xi}_2, \bar{\xi}_2] \times \cdots \times [\underline{\xi}_l, \bar{\xi}_l]$  such that  $\boldsymbol{\xi} \in \Omega$ , where  $l$  is the dimension of  $\boldsymbol{\xi}$ .

The assumption on Lipschitz continuity limits how fast the function  $h(\mathbf{x}, \boldsymbol{\xi})$  can change with respect to both  $\mathbf{x}$  and  $\boldsymbol{\xi}$ , and is an assumption often applied in simulation models that are studied in the operational research community, see [Fan and Hu \(2018\)](#), [Ghosh and Lam \(2019\)](#). The assumption of bounded support for  $\boldsymbol{\xi}$  holds for most simulation models. For example, in an inventory problem, the random demand is usually bounded.

To establish the consistency and asymptotic normality, we need the following lemma to transform the objective function given in Equation (4) into a summation of some independent and identically distributed (i.i.d.) terms. This summation representation allows us to



use results on the empirical process to analyze the asymptotic behavior of the estimators given by Equation (4). In this paper, all the theoretical proofs are provided in the electronic companion.

LEMMA 1. *Suppose Assumption 1 holds. Then*

$$\mathbb{E}_\pi[\mathbb{E}_P[h(\mathbf{x}, \boldsymbol{\xi})]] = \mathbb{E}_{P_0} \frac{\alpha}{\alpha + n} h(\mathbf{x}, \boldsymbol{\xi}) + \frac{1}{\alpha + n} \sum_{j=1}^n h(\mathbf{x}, \boldsymbol{\xi}_j). \quad (6)$$

Now we can prove the consistency and asymptotic normality given by the following two theorems. Put  $f(\mathbf{x}) = \mathbb{E}_{P^c}[h(\mathbf{x}, \boldsymbol{\xi})]$ . Suppose that  $\mathbf{x}_n = \arg \min_x \mathbb{E}_\pi[\mathbb{E}_P[h(\mathbf{x}, \boldsymbol{\xi})]]$  and  $\mathbf{x}^* = \arg \min_x \mathbb{E}_{P^c}[h(\mathbf{x}, \boldsymbol{\xi})] = \arg \min_x f(\mathbf{x})$ . The following Theorem 1 and Theorem 2 summarize the results of consistency and the asymptotic normality respectively. We use  $\rightarrow_p$  to denote the convergence in probability and  $\rightsquigarrow$  to denote the convergence in distribution.

THEOREM 1. *Suppose Assumption 1 holds. Then*

(i) *(Consistency of the value of the objective function) As  $n \rightarrow +\infty$ ,*

$$\mathbb{E}_\pi[\mathbb{E}_P[h(\mathbf{x}, \boldsymbol{\xi})]] \rightarrow_p \mathbb{E}_{P^c}[h(\mathbf{x}, \boldsymbol{\xi})].$$

(ii) *(Consistency of the optimal solution) Suppose  $\mathbf{x}^*$  is well separated, i.e.,*

$$\inf_{|\mathbf{x} - \mathbf{x}^*| \geq \epsilon} f(\mathbf{x}) > f(\mathbf{x}^*) \quad (7)$$

As  $n \rightarrow +\infty$ ,

$$\mathbf{x}_n \rightarrow_p \mathbf{x}^*.$$

(iii) *(Consistency of the optimal value)*

$$\mathbb{E}_\pi[\mathbb{E}_P[h(\mathbf{x}_n, \boldsymbol{\xi})]] \rightarrow_p \mathbb{E}_{P^c}[h(\mathbf{x}^*, \boldsymbol{\xi})].$$

THEOREM 2. *Suppose Assumption 1 holds, and further assume that  $\mathbb{E}_{P^c} \left( \frac{\partial h(\mathbf{x}^*, \boldsymbol{\xi})}{\partial \mathbf{x}} \right)^2$  exists and that  $f''(\mathbf{x}^*) = \frac{\partial^2 \mathbb{E}_{P^c}[h(\mathbf{x}^*, \boldsymbol{\xi})]}{\partial \mathbf{x}^2} \neq 0$ . Then*

(i) *(Asymptotic normality of the value of the objective function.) As  $n \rightarrow +\infty$ ,*

$$\sqrt{n} (\mathbb{E}_\pi[\mathbb{E}_P[h(\mathbf{x}, \boldsymbol{\xi})]] - \mathbb{E}_{P^c}[h(\mathbf{x}, \boldsymbol{\xi})]) \rightsquigarrow N(0, \sigma_{h(\mathbf{x})}^2),$$

where  $\sigma_{h(\mathbf{x})}^2 = \text{Var}(h(\mathbf{x}, \boldsymbol{\xi}))$ .

(ii) *(Asymptotic normality of the optimal solution)*

$$\sqrt{n}(\mathbf{x}_n - \mathbf{x}^*) \rightsquigarrow N(0, \sigma_x^2)$$

where  $\sigma_x^2 = \mathbb{E}_{P^c} \left( \frac{\partial h(\mathbf{x}^*, \boldsymbol{\xi})}{\partial \mathbf{x}} \right)^2 / (f''(\mathbf{x}^*))^2$ .

(iii) *(Asymptotic normality of the optimal value)* As  $n \rightarrow +\infty$ ,

$$\sqrt{n} (\mathbb{E}_\pi [\mathbb{E}_P [h(\mathbf{x}_n, \boldsymbol{\xi})]] - \mathbb{E}_{P^c} [h(\mathbf{x}^*, \boldsymbol{\xi})]) \rightsquigarrow N(0, \sigma_{h(\mathbf{x}^*)}^2),$$

where  $\sigma_{h(\mathbf{x}^*)}^2 = \text{Var}(h(\mathbf{x}^*, \boldsymbol{\xi}))$ .

REMARK 1. Our results coincide with the results in [Wu et al. \(2018\)](#) for a special case. Here, we consider an example when  $\boldsymbol{\xi}$  is a binary variable with  $P(\boldsymbol{\xi} = \boldsymbol{\xi}_1) = \theta^c$  and  $P(\boldsymbol{\xi} = \boldsymbol{\xi}_2) = 1 - \theta^c$ . According to our Theorem 2, we have  $\sqrt{n} (\mathbb{E}_\pi [\mathbb{E}_P [h(\mathbf{x}, \boldsymbol{\xi})]] - \mathbb{E}_{P^c} [h(\mathbf{x}, \boldsymbol{\xi})]) \rightsquigarrow N(0, \sigma_{h(\mathbf{x})}^2)$ , where  $\sigma_{h(\mathbf{x})}^2 = \text{Var}(h(\mathbf{x}, \boldsymbol{\xi})) = (\theta^c h^2(\mathbf{x}, \boldsymbol{\xi}_1) + (1 - \theta^c) h^2(\mathbf{x}, \boldsymbol{\xi}_2)) - (\theta^c h(\mathbf{x}, \boldsymbol{\xi}_1) + (1 - \theta^c) h(\mathbf{x}, \boldsymbol{\xi}_2))^2 = \theta^c (1 - \theta^c) (h(\mathbf{x}, \boldsymbol{\xi}_1) - h(\mathbf{x}, \boldsymbol{\xi}_2))^2$ .

Since  $\boldsymbol{\xi}$  is a binary random variable with parameter  $\theta_c$ , we apply the results in [Wu et al. \(2018\)](#). According to Theorem 4.4 of [Wu et al. \(2018\)](#),  $\sqrt{n} (\mathbb{E}_\pi [\mathbb{E}_P [h(\mathbf{x}, \boldsymbol{\xi})]] - \mathbb{E}_{P^c} [h(\mathbf{x}, \boldsymbol{\xi})]) \rightsquigarrow N(0, \sigma^2)$ , where  $\sigma^2 = (\partial_\theta \mathbb{E} h(\mathbf{x}, \boldsymbol{\xi}))^2 I(\theta^c)^{-1} = (\theta^c h(\mathbf{x}, \boldsymbol{\xi}_1) + (1 - \theta^c) h(\mathbf{x}, \boldsymbol{\xi}_2))_\theta^2 I(\theta^c)^{-1} = (h(\mathbf{x}, \boldsymbol{\xi}_1) - h(\mathbf{x}, \boldsymbol{\xi}_2))^2 I(\theta^c)^{-1} = \theta^c (1 - \theta^c) (h(\mathbf{x}, \boldsymbol{\xi}_1) - h(\mathbf{x}, \boldsymbol{\xi}_2))^2$  as  $I(\theta^c) = \frac{1}{\theta^c(1-\theta^c)}$  for binary variable  $\boldsymbol{\xi}$ . Hence, for this special case, our results for general nonparametric models recover the results of [Wu et al. \(2018\)](#). Furthermore, when  $\mathbf{x} = \mathbf{x}^*$ , we can also recover the asymptotic variance provided in Theorem 4.13 of [Wu et al. \(2018\)](#).

REMARK 2. [Wu et al. \(2018\)](#) assumes a parametric family for the input distribution and determines the asymptotic properties for four risk functions: the expectation, the mean-variance, the value-at-risk, and the conditional value-at-risk, while the present paper focuses on the expectation risk function with unknown parametric family for the input distribution. [Wu et al. \(2018\)](#) and the present paper both complete the proof of the consistency properties of the value of the objective function, the optimal solution, and the optimal value, as well as the asymptotic normality of the value of the objective function and the optimal value. In addition, we also provide here the proof of the asymptotic normality of the optimal solution, which is not covered by ([Wu et al. 2018](#)). The asymptotic normality of the optimal solution is important as it can help decision makers quantify

the uncertainties in the estimator for the optimal solution. The uncertainties are closely related to the trustworthiness of the solution: a large variance implies the estimator might be very different from the true optimal solution. The uncertainty can also be quantified using confidence intervals, where a large interval corresponds to high uncertainty. Further, linking the uncertainty to the size of real world dataset  $n$  will also allow decision makers to design the data collection scheme to control the error within their tolerance levels.

#### 4. An efficient approach to NBRO: an algorithm based on Gaussian process

It was shown in Section 3 that the NBRO problem is valid, and now we aim to propose an efficient algorithm to solve it. If we write the inner expectation in (4) as  $f(\mathbf{x}, \mathbf{P}) = \mathbb{E}_{\boldsymbol{\xi} \sim \mathbf{P}}[h(\mathbf{x}, \boldsymbol{\xi})]$ , then problem (4) is equivalent to

$$\min_x g(\mathbf{x}) = \mathbb{E}_{\mathbf{P} \sim \pi}[f(\mathbf{x}, \mathbf{P})], \quad (8)$$

where  $\mathbf{x} \in \mathbb{R}^d$ ,  $\boldsymbol{\xi} \in \mathbb{R}^l$ ,  $\boldsymbol{\xi} \sim \mathbf{P}$ , and  $\pi$  is a multidimensional Dirichlet process posterior. Here, we consider the case when the different dimensions of  $\boldsymbol{\xi}$  are independent, i.e., we consider independent univariate input distributions. In this case, the distribution of each dimension of  $\boldsymbol{\xi}$  can be modeled independently with a univariate Dirichlet process posterior  $P^{(i)}, i = 1, \dots, l$ , and then  $\mathbf{P} = P^{(1)} \times P^{(2)} \dots \times P^{(l)}$ . Note that  $f(\mathbf{x}, \mathbf{P})$  can only be estimated through noisy simulation outputs  $h(\mathbf{x}, \boldsymbol{\xi})$ . In addition, the design space  $\mathcal{X}$  is continuous. Hence it is impossible to evaluate all possible design–distribution points  $(\mathbf{x}, \mathbf{P})$  to get full information about the surface of  $f(\mathbf{x}, \mathbf{P})$ . Here we focus on the goal of making the best use of the finite simulation runs to solve (8). With a limited budget, algorithms based on Gaussian process (GP) have been shown to be efficient and effective in solving simulation optimization problems (Frazier 2018).

In order to use GP-based optimization algorithms to solve (8), a GP model for  $g(\mathbf{x})$  is required. Since the simulation budget is limited, we cannot estimate observations of  $g(\mathbf{x})$  with direct simulation methods (Chick 2001, Zouaoui and Wilson 2003) which require a large number of simulations at each design point. Therefore, the simulation output on  $g(\mathbf{x})$  is not readily available and only the simulation output on  $f(\mathbf{x}, \mathbf{P})$  is observable. In this case, we would like to first obtain a GP model as an approximate model for  $f(\mathbf{x}, \mathbf{P})$ , and develop an approximate model for  $g(\mathbf{x})$ . Then we apply this approximation of  $g(\mathbf{x})$  in the EGO algorithm to efficiently solve the problem (8).

#### 4.1. Stochastic GP model of $f(\mathbf{x}, \mathbf{P})$

Let  $y(\mathbf{x}, \mathbf{P}) \triangleq h(\mathbf{x}, \boldsymbol{\xi})$  be the stochastic simulation output at  $(\mathbf{x}, \mathbf{P})$ , and  $f(\mathbf{x}, \mathbf{P})$  be the mean function of the simulator. We assume that the simulation output  $y(\mathbf{x}, \mathbf{P})$  is a realization of a random process that can be described by the following model:

$$y(\mathbf{x}, \mathbf{P}) = F(\mathbf{x}, \mathbf{P}) + \epsilon. \quad (9)$$

The stochastic noise  $\epsilon$  is assumed to follow a normal distribution with mean 0 and finite constant variance, i.e.,  $\epsilon \sim \mathcal{N}(0, \sigma_\epsilon^2)$ . This assumption is appropriate for many simulation models as the outputs is often the average of many basic simulation outputs. The unknown mean response is modeled by a stochastic process  $F(\mathbf{x}, \mathbf{P})$ , which can be interpreted as the prior for the unknown mean function of the simulator.  $F(\mathbf{x}, \mathbf{P})$  is assumed to be a Gaussian process with mean  $l(\mathbf{x}, \mathbf{P})^\top \boldsymbol{\beta}$  and covariance function  $\Sigma_F$ , where  $l(\mathbf{x}, \mathbf{P})$  is a  $q \times 1$  vector of basic functions and  $\boldsymbol{\beta}$  is a  $q \times 1$  vector of trend parameters. The mean (also termed as trend)  $l(\mathbf{x}, \mathbf{P})^\top \boldsymbol{\beta}$  captures the global spatial information. The covariance function  $\Sigma_F$  is used to measure the local spatial correlation of  $F$  between any two points  $(\mathbf{x}, \mathbf{P})$  and  $(\mathbf{x}', \mathbf{P}')$ :  $\Sigma_F((\mathbf{x}, \mathbf{P}), (\mathbf{x}', \mathbf{P}')) = \text{Cov}(F(\mathbf{x}, \mathbf{P}), F(\mathbf{x}', \mathbf{P}')) = \tau^2 R_F((\mathbf{x}, \mathbf{P}), (\mathbf{x}', \mathbf{P}'); \theta)$ , where  $R_F$  is the correlation function with parameter  $\theta$  and  $\tau$  is the variance parameter.

If a Gaussian prior is additionally selected for  $\boldsymbol{\beta}$ , i.e.  $\boldsymbol{\beta} \sim \mathcal{N}(\mathbf{b}, \Omega)$ , with appropriately chosen  $\mathbf{b}$  and  $\Omega$ , then stochastic process  $F(\mathbf{x}, \mathbf{P})$  used to model the mean function is

$$F(\mathbf{x}, \mathbf{P}) \sim GP(l(\mathbf{x}, \mathbf{P})^\top \mathbf{b}, l(\mathbf{x}, \mathbf{P})^\top \Omega l(\mathbf{x}, \mathbf{P}) + \tau^2 R_F((\mathbf{x}', \mathbf{P}'), (\mathbf{x}', \mathbf{P}'); \theta)) \quad (10)$$

The metamodel is flexible enough to encompass different types of prior information about the mean response (Xie et al. 2014). The global spatial information can be incorporated by choosing the basis functions  $l(\mathbf{x}, \mathbf{P})$  and the prior over  $\boldsymbol{\beta}$ . The local spatial correlation can be represented by the covariance function  $\tau^2 R_F((\mathbf{x}', \mathbf{P}'), (\mathbf{x}', \mathbf{P}'); \theta)$ .

Suppose the initial sample size is  $r \cdot s$ , i.e., we can evaluate  $f(\mathbf{x}, \mathbf{P})$  through simulation at  $s$  design–distribution pairs, and denote them by  $\{(\mathbf{x}_1, \mathbf{P}_1), \dots, (\mathbf{x}_s, \mathbf{P}_s)\}$ . At each sample design–distribution pair,  $r$  replicates of the simulation are conducted. Denote the simulation output at  $(\mathbf{x}_i, \mathbf{P}_i)$  for the  $j$ th simulation replicate by  $y_j(\mathbf{x}_i, \mathbf{P}_i)$ . The simulation output sample mean is then  $\bar{y}(\mathbf{x}_i, \mathbf{P}_i) = \frac{1}{r} \sum_{j=1}^r y_j(\mathbf{x}_i, \mathbf{P}_i)$ , and the observed simulation output sample mean vector is  $\bar{\mathbf{Y}}_s = \{\bar{y}(\mathbf{x}_1, \mathbf{P}_1), \dots, \bar{y}(\mathbf{x}_s, \mathbf{P}_s)\}$ . Given the simulation results of

$\bar{\mathbf{Y}}_s = \{\bar{y}(\mathbf{x}_1, \mathbf{P}_1), \dots, \bar{y}(\mathbf{x}_s, \mathbf{P}_s)\}$ , our belief about  $F$  can be updated. If the parameters  $\tau$  and  $\boldsymbol{\theta}$  are known, the posterior distribution  $F_s(\mathbf{x}, \mathbf{P}) \triangleq F | \bar{\mathbf{Y}}_s \sim \text{GP}(m_s, k_s)$  can be obtained, where  $m_s$  and  $k_s$  are the mean and covariance function of the GP  $F_s(\mathbf{x}, \mathbf{P})$  respectively:

$$m_s(\mathbf{x}, \mathbf{P}) = l(\mathbf{x}, \mathbf{P})^\top \hat{\boldsymbol{\beta}} + \tau^2 R_F((\mathbf{x}, \mathbf{P}), \cdot; \boldsymbol{\theta})^\top [\tau^2 \mathbf{R}_F(\boldsymbol{\theta}) + \boldsymbol{\Sigma}_\epsilon]^{-1} (\bar{\mathbf{Y}}_s - \mathbf{L}^\top \hat{\boldsymbol{\beta}}) \quad (11)$$

$$k_s((\mathbf{x}, \mathbf{P}), (\mathbf{x}', \mathbf{P}')) = \tau^2 R_F((\mathbf{x}, \mathbf{P}), (\mathbf{x}', \mathbf{P}'); \boldsymbol{\theta}) - \tau^4 \mathbf{R}_F((\mathbf{x}, \mathbf{P}), \cdot; \boldsymbol{\theta})^\top [\tau^2 \mathbf{R}_F(\boldsymbol{\theta}) + \boldsymbol{\Sigma}_\epsilon]^{-1} \mathbf{R}_F((\mathbf{x}', \mathbf{P}'), \cdot; \boldsymbol{\theta}) \\ + \eta(\mathbf{x}, \mathbf{P})^\top [\boldsymbol{\Omega}^{-1} + \mathbf{L}[\tau^2 \mathbf{R}_F(\boldsymbol{\theta}) + \boldsymbol{\Sigma}_\epsilon]^{-1} \mathbf{L}^\top]^{-1} \eta(\mathbf{x}', \mathbf{P}') \quad (12)$$

where  $\mathbf{L}$  is a  $q \times s$  matrix that collects the  $l(\mathbf{x}, \mathbf{P})$  vectors for all  $s$  observed points,  $\hat{\boldsymbol{\beta}} = (\boldsymbol{\Omega}^{-1} + \mathbf{L}(\tau^2 \mathbf{R}_F(\boldsymbol{\theta}) + \boldsymbol{\Sigma}_\epsilon)^{-1} \mathbf{L}^\top)^{-1} (\mathbf{L}(\tau^2 \mathbf{R}_F(\boldsymbol{\theta}) + \boldsymbol{\Sigma}_\epsilon)^{-1} \bar{\mathbf{Y}}_s + \boldsymbol{\Omega}^{-1} \mathbf{b})$  and  $\eta(\mathbf{x}, \mathbf{P}) = l(\mathbf{x}, \mathbf{P}) - \mathbf{L}(\tau^2 \mathbf{R}_F(\boldsymbol{\theta}) + \boldsymbol{\Sigma}_\epsilon)^{-1} \tau^2 \mathbf{R}_F((\mathbf{x}, \mathbf{P}), \cdot; \boldsymbol{\theta})$  (Rasmussen 2004). The posterior mean  $m_s$  can be used to approximate  $f(\mathbf{x}, \mathbf{P})$ .  $k_s((\mathbf{x}, \mathbf{P}), (\mathbf{x}', \mathbf{P}'))$  is the posterior covariance between any two design-distribution pairs, and the posterior variance of  $F$  is  $\mathcal{S}_s^2(\mathbf{x}, \mathbf{P}) = k_s((\mathbf{x}, \mathbf{P}), (\mathbf{x}, \mathbf{P}))$ . In addition,  $\tau^2 \mathbf{R}_F((\mathbf{x}, \mathbf{P}), \cdot; \boldsymbol{\theta})^\top = [\text{Cov}[F((\mathbf{x}, \mathbf{P})), F((\mathbf{x}_1, \mathbf{P}_1))], \dots, \text{Cov}[F((\mathbf{x}, \mathbf{P})), F((\mathbf{x}_s, \mathbf{P}_s))]]^\top$  is an  $s \times 1$  vector, and  $\tau^2 \mathbf{R}_F(\boldsymbol{\theta})$  is the  $s \times s$  covariance matrix across the  $s$  observed points, and  $\boldsymbol{\Sigma}_\epsilon = \text{Diag}\{\frac{1}{r} \sigma_\epsilon^2 \dots, \frac{1}{r} \sigma_\epsilon^2\} = \frac{1}{r} \sigma_\epsilon^2 \mathbf{I}$  is an  $s \times s$  matrix. If there is no prior knowledge about the trend, which is often case (as our experiments in Section 5), then a constant value  $l(\mathbf{x}, \mathbf{P})^\top \boldsymbol{\beta} = \beta_0$  is commonly used (Xie et al. 2014, Ankenman et al. 2010). In addition, a vague prior is imposed on  $\beta_0$ , i.e  $\beta_0 \sim N(0, \Omega)$ , where the  $\Omega^{-1} \rightarrow 0$ . In this case, the metamodel becomes the nugget-effect model (Cressie 1992).

The parameters  $\tau$ ,  $\boldsymbol{\theta}$  and  $\sigma_\epsilon^2$  in the metamodel are unknown and need to be estimated. One common approach is to estimate  $\tau$ , and  $\boldsymbol{\theta}$  with the maximum log-likelihood method (Rasmussen 2004, Ankenman et al. 2010), and to use the pooled variance of the simulation outputs to estimate  $\sigma_\epsilon^2$ . Another approach is to impose prior distributions on the parameters and model the parameter uncertainty with a hierarchical Bayesian framework, see Ng and Yin (2012), but this would increase the computational efforts.

For the stochastic GP model  $F_s(\mathbf{x}, \mathbf{P})$ , we also need to properly define or choose the correlation function between  $(\mathbf{x}, \mathbf{P})$  and  $(\mathbf{x}', \mathbf{P}')$ . We assume  $\mathbf{x}$  and  $\mathbf{P}$  are independent of each other. Denote the correlation function by  $R_F((\mathbf{x}, \mathbf{P}), (\mathbf{x}', \mathbf{P}')) = r_{\mathcal{X}}(\mathbf{x}, \mathbf{x}') r_{\mathcal{M}}(\mathbf{P}, \mathbf{P}')$ , where  $r_{\mathcal{X}}(\mathbf{x}, \mathbf{x}')$  and  $r_{\mathcal{M}}(\mathbf{P}, \mathbf{P}')$  are correlation kernels. The correlation kernels need to be symmetric and positive definite. For  $r_{\mathcal{X}}(\mathbf{x}, \mathbf{x}')$ , there are many choices, including the squared exponential, Matern correlation kernels, etc. In this article, we adopt the

most widely-used squared exponential correlation kernels (Rasmussen 2004):  $r_{\mathcal{X}}(\mathbf{x}, \mathbf{x}') = \exp\{-\sum_{i=1}^d \frac{(x_i - x'_i)^2}{2\theta_{1,i}^2}\}$ , where  $\theta_{1,i}, i = 1, \dots, d$  are length scale parameters. For  $r_{\mathcal{M}}(\mathbf{P}, \mathbf{P}')$ , we use the form  $r_{\mathcal{M}}(\mathbf{P}, \mathbf{P}') = \exp\{-\sum_{j=1}^l \frac{D^2(P^{(j)}, P^{(j)'})}{2\theta_{2,j}^2}\}$ , where  $D^2(P^{(j)}, P^{(j)'})$  is some measure of the distance between the input distributions  $P^{(j)}$  and  $P^{(j)'}$ , and  $\theta_{2,i}, i = 1, \dots, l$  are length scale parameters. In order to make the GP model valid, the measure of the distance between distributions  $D^2(\cdot, \cdot)$  need to result in positive definite correlation kernel.

There are several candidates satisfying this property, such as the total variation, the squared Hellinger distance, the Jensen–Shannon divergence (these three measures are  $f$ -divergence measures proposed by Hein and Bousquet (2004) and Fuglede and Topsoe (2004)), and the quadratic Wasserstein distance (Bachoc et al. 2017). In this paper, we choose the Wasserstein distance instead of the three  $f$ -divergence measures for the following reasons. The  $f$ -divergence measures only consider the pointwise difference between the input distributions, while the Wasserstein distance considers both the mass difference pointwise and the difference between points. Here we use a simple example for illustration. Consider the three distributions denoted by  $A$ ,  $B$ , and  $C$  in Figure 1. The distance between  $B$  and  $A$  and the distance between  $C$  and  $A$  are the same in terms of the three  $f$ -divergence measures, whereas the Wasserstein distance between  $C$  and  $A$  is larger than the Wasserstein distance between  $B$  and  $A$ . Intuitively, the Wasserstein distance is more reasonable as the characteristics of the distribution differs more between  $C$  and  $A$ , where the difference between the mean values of  $C$  and  $A$  ( $4 - 2 = 2$ ) is larger than that between  $B$  and  $A$  ( $2.5 - 2 = 0.5$ ) and the difference between the median values of  $C$  and  $A$  ( $5 - 1 = 4$ ) is also larger than that between  $B$  and  $A$  ( $2.5 - 2 = 0.5$ ). In short, the Wasserstein distance considers the whole shape of the distribution, and thus provides a more reasonable measure of the distance between distributions. In addition, we conducted a side experiment by constructing GP models based on the three  $f$ -divergence measures and the Wasserstein distance in order to compare their fitting performance with an inventory simulator (see details of the simulator in Section 5). The GP model based on Wasserstein distance outperforms the three  $f$ -divergence measures in terms of both mean loglikelihood and mean absolute error with leave-one-out cross validation over 100 macroreplications.

Formally, the quadratic Wasserstein distance between two univariate distributions  $Q$  and  $Q'$ , denoted by  $WD(Q, Q')$ , is defined by  $D^2(Q, Q') = WD(Q, Q') = \inf_{\tau \in \gamma(Q, Q')} E_{(z, z') \sim \tau} [|z - z'|^2]$ , where  $\gamma(Q, Q')$  is set of the joint distributions of  $(z, z')$  whose

marginal distributions are  $Q$  and  $Q'$ . The Wasserstein distance between two univariate distributions can be calculated efficiently with the algorithm provided by [Peyré et al. \(2019\)](#).

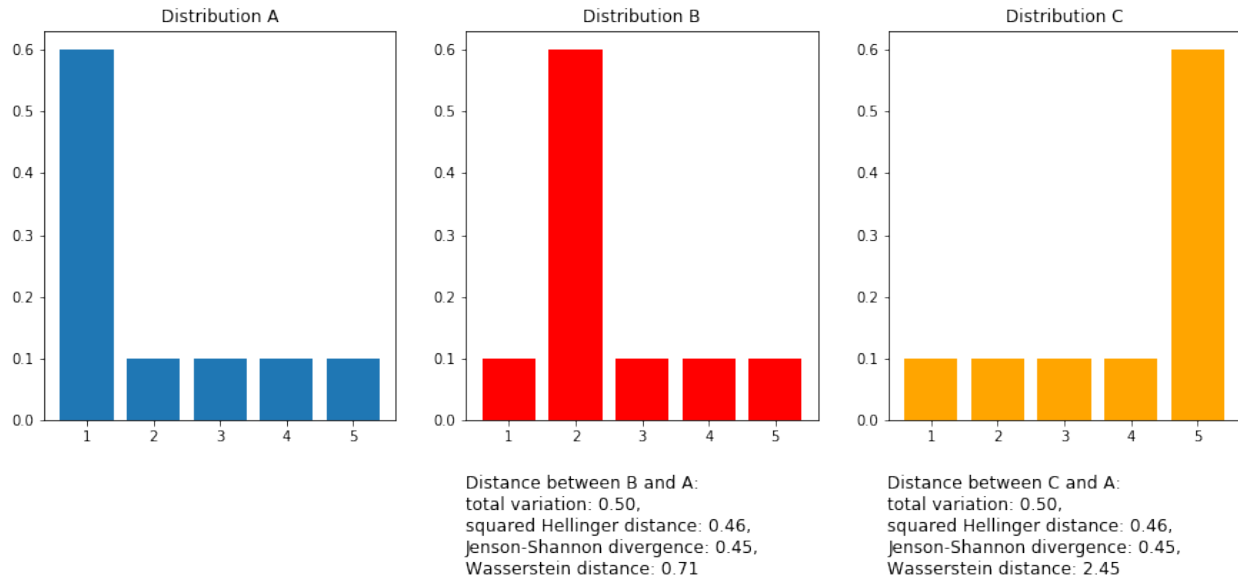


**Figure 1** Comparison of Wasserstein distance and the three  $f$ -divergence measures

## 4.2. Approximate model for $g(\mathbf{x})$

With  $F_s(\mathbf{x}, \mathbf{P})$  as the approximate model for  $f(\mathbf{x}, \mathbf{P})$ , we aim to derive the approximate model for  $g(\mathbf{x}) = \mathbb{E}_{\mathbf{P} \sim \pi}[f(\mathbf{x}, \mathbf{P})]$ . Specifically, we consider the following process:

$$G_s(\mathbf{x}) = \mathbb{E}_{\mathbf{P} \sim \pi}[F_s(\mathbf{x}, \mathbf{P})]. \quad (13)$$

By rewriting (13) as the limit of Riemann sums ([De Oliveira and Kone 2015](#)), it can be shown that  $G_s(\mathbf{x})$  is still a GP. The mean and covariance of  $G_s(\mathbf{x})$  can be derived as follows.

$$\mathbb{E}[G_s(\mathbf{x})] = \int_{\mathbf{P}} \mathbb{E}[F_s(\mathbf{x}, \mathbf{P})] \cdot \pi(\mathbf{P} | \mathbf{D}_n) d\mathbf{P} = \int_{\mathbf{P}} m_s(\mathbf{x}, \mathbf{P}) \cdot \pi(\mathbf{P} | \mathbf{D}_n) d\mathbf{P} \quad (14)$$

$$\text{Cov}[G_s(\mathbf{x}), G_s(\mathbf{x}')] = \int_{\mathbf{P}} \int_{\mathbf{P}'} \pi(\mathbf{P} | \mathbf{D}_n) \pi(\mathbf{P}' | \mathbf{D}_n) k_s((\mathbf{x}, \mathbf{P}), (\mathbf{x}', \mathbf{P}')) d\mathbf{P}' d\mathbf{P} \quad (15)$$

The integrals in (14) and (15) can be estimated numerically through Monte Carlo (MC) techniques. Specifically,  $N_{MC}$  samples of  $\{\mathbf{P}_1, \dots, \mathbf{P}_{N_{MC}}\}$  can be generated from  $\pi(\mathbf{P} | \mathbf{D}_n)$  to compute

$$\mathbb{E}[G_s(\mathbf{x})] \approx \mu_s(\mathbf{x}) = \frac{1}{N_{MC}} \sum_{i=1}^{N_{MC}} m_s(\mathbf{x}, \mathbf{P}_i) \quad (16)$$

$$\text{Cov}[G_s(\mathbf{x}), G_s(\mathbf{x}')] \approx c_s(\mathbf{x}, \mathbf{x}') = \frac{1}{N_{MC}^2} \sum_{i=1}^{N_{MC}} \sum_{j=1}^{N_{MC}} k_s((\mathbf{x}, \mathbf{P}_i), (\mathbf{x}', \mathbf{P}_j)) \quad (17)$$

$\text{Var}[G_s(\mathbf{x})] \approx \sigma_s^2(\mathbf{x}) = c_s(\mathbf{x}, \mathbf{x})$ . In fact, we have  $\mu_s(\mathbf{x}) = \mathbb{E} \left[ \frac{1}{N_{MC}} \sum_{i=1}^{N_{MC}} F_s(\mathbf{x}, \mathbf{P}_i) \right]$  and  $c_s(\mathbf{x}, \mathbf{x}') = \text{Cov}(\frac{1}{N_{MC}} \sum_{i=1}^{N_{MC}} F_s(\mathbf{x}, \mathbf{P}_i), \frac{1}{N_{MC}} \sum_{j=1}^{N_{MC}} F_s(\mathbf{x}', \mathbf{P}_j))$ . Furthermore, as

$$\hat{G}_s(\mathbf{x}) = \frac{1}{N_{MC}} \sum_{i=1}^{N_{MC}} F_s(\mathbf{x}, \mathbf{P}_i) \quad (18)$$

is a finite sum of Gaussian random variables,  $\hat{G}_s(\mathbf{x})$  is a Gaussian process with mean  $\mu_s(\mathbf{x})$  and covariance  $c_s(\mathbf{x}, \mathbf{x}')$ . The above  $\hat{G}_s(\mathbf{x})$  can then be used to approximate  $G_s(\mathbf{x})$  and used as the approximate model for  $g(\mathbf{x})$ . Then  $\hat{G}_s(\mathbf{x})$  is our current knowledge about the surface of  $g(\mathbf{x})$  after the initial evaluations. The MC samples  $\mathbf{P}_i$  in (18) are generated from the posterior  $\boldsymbol{\pi}$ . Popular sampling methods, such as the algorithm of the stick-breaking process (Hjort et al. 2010), can be used to generate the samples  $\mathbf{P}_i$  efficiently.

### 4.3. EGO with Input Uncertainty to Select $(\mathbf{x}_{s+1}, \mathbf{P}_{s+1})$

In this section, we aim to modify EGO, a popular global optimization algorithm first proposed by Jones et al. (1998), to guide the selection of  $(\mathbf{x}_{s+1}, \mathbf{P}_{s+1})$  for the next evaluation.

**4.3.1. Overview of EGO** EGO was first introduced to solve the deterministic simulation optimization problem when the simulation outputs are deterministic. EGO starts by evaluating at an initial set of evaluation points to estimate a GP model and then takes sequential steps to search the space. The subsequent evaluation point is determined by maximizing the expected improvement of the new function evaluation over the current best evaluations, which is defined as the Expectation Improvement (EI) criterion calculated based on the GP model. The EI criterion not only aims to choose points that can reduce the value of the objective function the most, but also considers the uncertainty at unobserved points, enabling it to balance the search within local areas of current optimum and unexplored areas away from previously observed points. The optimum is finally determined by the minimum of the simulation output at the already sampled points.

**4.3.2. Modified EGO with input uncertainty algorithm** In order to adapt the EGO for the stochastic optimization problem and take into account the input uncertainty to solve (8), we need to answer two questions: what are the current best values of  $g(\mathbf{x})$  and what is the predictive distribution of  $g(\mathbf{x})$  after a new hypothetical evaluation is generated?



Recall that in Section 4.2, we derived a GP model  $\hat{G}_s(\mathbf{x})$  for  $g(\mathbf{x})$  with the predictive mean being  $\mu_s(\mathbf{x})$ . Here, we estimate the current best values upon which we aim to improve, denoted by  $T$ , as the the best predictive mean  $\mu(x)$  over the already sampled design points, i.e.,  $T = \min\{\mu_s(\mathbf{x}_1), \dots, \mu_s(\mathbf{x}_s)\}$ .

To answer the second question, we need to derive the predictive distribution  $\hat{G}_{s+1}(\mathbf{x})$  conditional on the evaluation at an arbitrary point  $(\mathbf{x}_{s+1}, \mathbf{P}_{s+1})$ , denoted by  $\hat{G}_{s+1}(\mathbf{x}|\mathbf{x}_{s+1}, \mathbf{P}_{s+1})$ . Before obtaining the predictive distribution  $\hat{G}_{s+1}(\mathbf{x}|\mathbf{x}_{s+1}, \mathbf{P}_{s+1})$ , we need to first derive the predictive distribution  $F_{s+1}(\mathbf{x}, \mathbf{P})$  conditional on evaluation at  $(\mathbf{x}_{s+1}, \mathbf{P}_{s+1})$ , denoted by  $F_{s+1}((\mathbf{x}, \mathbf{P}_i)|\mathbf{x}_{s+1}, \mathbf{P}_{s+1})$ . Then we have

$$\hat{G}_{s+1}(\mathbf{x}|\mathbf{x}_{s+1}, \mathbf{P}_{s+1}) = \frac{1}{N_{mc}} \sum_{i=1}^{N_{mc}} F_{s+1}((\mathbf{x}, \mathbf{P}_i)|\mathbf{x}_{s+1}, \mathbf{P}_{s+1}). \quad (19)$$

Suppose we denote the value evaluated at  $(\mathbf{x}_{s+1}, \mathbf{P}_{s+1})$  by  $y_{s+1}$ . Conditioning on this value, we can derive the conditional distribution  $F_{s+1}((\mathbf{x}, \mathbf{P})|\mathbf{x}_{s+1}, \mathbf{P}_{s+1}, y_{s+1}) \sim GP(m'_{s+1}, k'_{s+1})$  with the following mean and covariance:

$$\begin{aligned} m'_{s+1}(\mathbf{x}, \mathbf{P}) &= m_s(\mathbf{x}, \mathbf{P}) + \frac{k_s((\mathbf{x}, \mathbf{P}), (\mathbf{x}_{s+1}, \mathbf{P}_{s+1}))}{k_s((\mathbf{x}_{s+1}, \mathbf{P}_{s+1}), (\mathbf{x}_{s+1}, \mathbf{P}_{s+1})) + \frac{1}{r}\sigma_\epsilon^2} [y_{s+1} - m_s(\mathbf{x}, \mathbf{P})] \\ &= m_s(\mathbf{x}, \mathbf{P}) + \frac{k_s((\mathbf{x}, \mathbf{P}), (\mathbf{x}_{s+1}, \mathbf{P}_{s+1}))}{\sqrt{k_s((\mathbf{x}_{s+1}, \mathbf{P}_{s+1}), (\mathbf{x}_{s+1}, \mathbf{P}_{s+1})) + \frac{1}{r}\sigma_\epsilon^2}} Z, \end{aligned} \quad (20)$$

$$k'_{s+1}((\mathbf{x}, \mathbf{P}), (\mathbf{x}', \mathbf{P}')) = k_s((\mathbf{x}, \mathbf{P}), (\mathbf{x}', \mathbf{P}')) - \frac{k_s((\mathbf{x}, \mathbf{P}), (\mathbf{x}_{s+1}, \mathbf{P}_{s+1}))k_s((\mathbf{x}', \mathbf{P}'), (\mathbf{x}_{s+1}, \mathbf{P}_{s+1}))}{k_s((\mathbf{x}_{s+1}, \mathbf{P}_{s+1}), (\mathbf{x}_{s+1}, \mathbf{P}_{s+1})) + \frac{1}{r}\sigma_\epsilon^2}, \quad (21)$$

where  $Z \sim \mathcal{N}(0, 1)$  is a standard normal random variable.

Then from Equation (19), we can obtain the distribution of  $\hat{G}_{s+1}(\mathbf{x}|\mathbf{x}_{s+1}, \mathbf{P}_{s+1}, y_{s+1})$ , whose conditional mean and covariance can be derived as

$$\begin{aligned} \mathbb{E} \left[ \hat{G}_{s+1}(\mathbf{x}|\mathbf{x}_{s+1}, \mathbf{P}_{s+1}, y_{s+1}) \right] &= \frac{1}{N_{mc}} \sum_{i=1}^{N_{mc}} m'_{s+1}(\mathbf{x}, \mathbf{P}_i) \\ &= \frac{1}{N_{mc}} \sum_{i=1}^{N_{mc}} m_s(\mathbf{x}, \mathbf{P}_i) + Z \frac{1}{N_{mc}} \sum_{i=1}^{N_{mc}} \frac{k_s((\mathbf{x}, \mathbf{P}_i), (\mathbf{x}_{s+1}, \mathbf{P}_{s+1}))}{\sqrt{k_s((\mathbf{x}_{s+1}, \mathbf{P}_{s+1}), (\mathbf{x}_{s+1}, \mathbf{P}_{s+1})) + \frac{1}{r}\sigma_\epsilon^2}} \\ &\sim \mathcal{N} \left( \frac{1}{N_{mc}} \sum_{i=1}^{N_{mc}} m_s(\mathbf{x}, \mathbf{P}_i), \left( \frac{1}{N_{mc}} \sum_{i=1}^{N_{mc}} \frac{k_s((\mathbf{x}, \mathbf{P}_i), (\mathbf{x}_{s+1}, \mathbf{P}_{s+1}))}{\sqrt{k_s((\mathbf{x}_{s+1}, \mathbf{P}_{s+1}), (\mathbf{x}_{s+1}, \mathbf{P}_{s+1})) + \frac{1}{r}\sigma_\epsilon^2}} \right)^2 \right), \end{aligned} \quad (22)$$

$$\text{Cov}[\hat{G}_{s+1}(\mathbf{x}|\mathbf{x}_{s+1}, \mathbf{P}_{s+1}, y_{s+1}), \hat{G}_{s+1}(\mathbf{x}'|\mathbf{x}_{s+1}, \mathbf{P}_{s+1}, y_{s+1})] = \frac{1}{N_{mc}^2} \sum_{i=1}^{N_{mc}} \sum_{j=1}^{N_{mc}} k'_{s+1}((\mathbf{x}, \mathbf{P}_i), (\mathbf{x}', \mathbf{P}_j)). \quad (23)$$

It can then be derived that  $\hat{G}_{s+1}(\mathbf{x}|\mathbf{x}_{s+1}, \mathbf{P}_{s+1}) \sim \mathcal{N}(\mu'_s(\mathbf{x}), \sigma_s'^2(\mathbf{x}))$ , where

$$\mu'_s(\mathbf{x}) = \frac{1}{N_{mc}} \sum_{i=1}^{N_{mc}} m_s(\mathbf{x}, \mathbf{P}_i), \quad (24)$$

$$\sigma_s^2(\mathbf{x}) = \left( \frac{1}{N_{mc}} \sum_{i=1}^{N_{mc}} \frac{k_s((\mathbf{x}, \mathbf{P}_i), (\mathbf{x}_{s+1}, \mathbf{P}_{s+1}))}{\sqrt{k_s((\mathbf{x}_{s+1}, \mathbf{P}_{s+1}), (\mathbf{x}_{s+1}, \mathbf{P}_{s+1})) + \frac{1}{r} \sigma_\epsilon^2}} \right)^2 + \frac{1}{N_{mc}^2} \sum_{i=1}^{N_{mc}} \sum_{j=1}^{N_{mc}} k'_{s+1}((\mathbf{x}, \mathbf{P}_i), (\mathbf{x}, \mathbf{P}_j)). \quad (25)$$

If we only consider the updated value at  $\mathbf{x}_{s+1}$  resulting from a new evaluation at  $(\mathbf{x}_{s+1}, \mathbf{P}_{s+1})$ , then the expected improvement over the current best values, the proposed EI based infill criterion, is given by

$$\begin{aligned} \text{EI}_T(\mathbf{x}_{s+1}, \mathbf{P}_{s+1}) &= \mathbb{E}_{\hat{G}_{s+1}} [(T - \hat{G}_{s+1}(\mathbf{x}_{s+1} | \mathbf{x}_{s+1}, \mathbf{P}_{s+1}))^+ | \bar{\mathbf{Y}}_s] \\ &= \Delta \Phi \left( \frac{\Delta}{\sigma'_s(\mathbf{x}_{s+1})} \right) + \sigma'_s(\mathbf{x}_{s+1}) \phi \left( \frac{\Delta}{\sigma'_s(\mathbf{x}_{s+1})} \right) \end{aligned} \quad (26)$$

where  $\Delta = T - \mu'_s(\mathbf{x}_{s+1})$  and  $T$  is the approximated current best value for  $g(\mathbf{x})$ . Although the value of  $g(\mathbf{x}_{s+1})$  is unknown, we have derived an approximation given by the distribution  $\hat{G}_{s+1}(\mathbf{x}_{s+1} | \mathbf{x}_{s+1}, \mathbf{P}_{s+1})$ . Hence, the improvement given by  $T - \hat{G}_{s+1}(\mathbf{x}_{s+1} | \mathbf{x}_{s+1}, \mathbf{P}_{s+1})$  is averaged with respect to the marginal distribution  $\hat{G}_{s+1}(\mathbf{x}_{s+1} | \mathbf{x}_{s+1}, \mathbf{P}_{s+1})$ . Since  $\hat{G}_{s+1}(\mathbf{x}_{s+1} | \mathbf{x}_{s+1}, \mathbf{P}_{s+1})$  is a normal random variable, the EI function can be computed analytically.

The next design–distribution pair is selected with  $\arg \max_{(\mathbf{x}_{s+1}, \mathbf{P}_{s+1})} \text{EI}_T(\mathbf{x}_{s+1}, \mathbf{P}_{s+1})$ , i.e., the point that can on average improve the objective function value most is selected. We then use  $r$  simulation replications to evaluate on the point  $(\mathbf{x}_{s+1}, \mathbf{P}_{s+1})$  to obtain the simulation output  $\bar{y}(\mathbf{x}_{s+1}, \mathbf{P}_{s+1})$ . The GP model is updated and next evaluation point is selected again based on the above EI criterion. This way of selecting evaluation points is iterated until the total simulation budget  $N \times r$  is exhausted. Denote  $\mathcal{V}_N = \{\mathbf{x}_1, \dots, \mathbf{x}_n\}$ , the set of all design points visited by the time the budget has been exhausted. The minimizer of the predictive mean  $\mu_N(\mathbf{x})$  of  $\hat{G}_N(\cdot)$  over the  $\mathcal{V}_N$  is returned as the final approximate minimizer, i.e.,  $\hat{\mathbf{x}}^* = \arg \min_{\mathbf{x} \in \mathcal{V}_N} \mu_N(\mathbf{x})$ . As more and more points are evaluated, the approximate model  $\hat{G}(\cdot)$  can better and better approximate the objective function  $g(\mathbf{x})$ , and consequently the accuracy of the approximation of  $\hat{\mathbf{x}}^*$  is also improved. Algorithm 1 below outlines the general steps of our proposed algorithm.

**REMARK 3.** In the present paper, we have modified the EGO algorithm to consider the input uncertainty. Other GP-based algorithms, such as Sequential Kriging Optimization (Huang et al. 2006), Knowledge Gradient (Frazier et al. 2009), Informational Approach to Global Optimization (Villemonteix et al. 2009), Expected Excursion Volume (Picheny 2015) can also be adapted and adjusted for input uncertainty. Here, we use EGO as it is

---

**Algorithm 1** Modified EGO Algorithm with Input Uncertainty

---

- 1: Given i.i.d. real world data  $\mathbf{D}_n = \{\boldsymbol{\xi}_1, \boldsymbol{\xi}_2, \dots, \boldsymbol{\xi}_n\}$  of size  $n$  and the Dirichlet process prior  $DP(\alpha, \mathbf{P}_0)$  on the input distribution  $\mathbf{P}$ , derive the posterior  $\pi(\mathbf{P}|\mathbf{D}_n)$ ;
  - 2: **Initialization:** Generate  $\{\mathbf{x}_1, \mathbf{x}_2, \dots, \mathbf{x}_s\}$  using Latin Hypercube Sampling from the uniform distribution with support  $\mathcal{X}$  and generate  $\{\mathbf{P}_1, \mathbf{P}_2, \dots, \mathbf{P}_s\}$  randomly from  $\pi(\mathbf{P}|\mathbf{D}_n)$  to obtain an initial set of design–distribution sample pairs  $\{(\mathbf{x}_1, \mathbf{P}_1), (\mathbf{x}_2, \mathbf{P}_2), \dots, (\mathbf{x}_s, \mathbf{P}_s)\}$ . Let  $\mathcal{V}_s = \{\mathbf{x}_1, \dots, \mathbf{x}_s\}$ , the set of all design points visited;
  - 3: Run the simulation experiment at these initial sample points with  $r$  replications at each point and obtain the observed output sample mean vector  $\bar{\mathbf{Y}}_s = [\bar{y}(\mathbf{x}_1, \mathbf{P}_1), \bar{y}(\mathbf{x}_2, \mathbf{P}_2), \dots, \bar{y}(\mathbf{x}_s, \mathbf{P}_s)]^T$ ;
  - 4: **Validation:** Based on  $\bar{\mathbf{Y}}_s$ , construct a stochastic GP model  $F_s(\mathbf{x}, \mathbf{P})$ ; Perform cross-validation (e.g., Leave-one-out cross validation) to ensure that the metamodel is valid;
  - 5: **while**  $s \leq N - 1$  **do**  $\triangleright N \times r$  is the total budget
  - 6:     Generate  $\mathbf{P}_1, \dots, \mathbf{P}_{N_{MC}}$  from  $\pi(\mathbf{P}|\mathbf{D}_n)$ ; Derive the model  $\hat{G}_s(\mathbf{x}, \mathbf{P}) \sim \text{GP}(\mu_s, c_s)$  for  $g(\mathbf{x})$ ;
  - 7:     **Selection:** Choose the subsequent design–distribution point  $(\mathbf{x}_{s+1}, \mathbf{P}_{s+1})$  that maximizes  $\text{EI}_T(\mathbf{x}_{s+1}, \mathbf{P}_{s+1})$  in Equation (26);
  - 8:     Run simulation experiments at  $(\mathbf{x}_{s+1}, \mathbf{P}_{s+1})$  with  $r$  replications and obtain the observed output mean  $\bar{y}(\mathbf{x}_{s+1}, \mathbf{P}_{s+1})$ , set  $\bar{\mathbf{Y}}_{s+1} = [\bar{\mathbf{Y}}_s, \bar{y}(\mathbf{x}_{s+1}, \mathbf{P}_{s+1})]^T$ ;
  - 9:     **Update:** update the stochastic GP model  $F_s(\mathbf{x}, \mathbf{P})$  based on  $\bar{\mathbf{Y}}_{s+1}$ ;
  - 10:     Set  $\mathcal{V}_{s+1} = \mathcal{V}_s \cup \mathbf{x}_{s+1}$  and set  $s = s + 1$ ;
  - 11: **return**  $\hat{\mathbf{x}}^* = \arg \min_{\mathbf{x} \in \mathcal{V}_N} \mu_N(\mathbf{x})$ .
- 

straightforward to calculate and is the most commonly used GP-based simulation optimization algorithm.

**4.3.3. Convergence analysis of the modified EGO algorithm** In this section, we aim to study the convergence of our modified EGO algorithm. The modified EGO algorithm is proposed to find the optimal value of the NBRO problem. Here, we aim to show that 1) the NBRO problem in Equation (4) can be well-solved by our proposed algorithm when the number of real world data points  $n$  is fixed and the simulation budget  $N$  goes to infinity; 2) if both  $n$  and  $N$  goes to infinity, the estimated optimal value/solution

would converge to the optimal value/solution of the true problem in Equation (1). We first introduce our main assumptions.

ASSUMPTION 2.  $\mathcal{X}$  is a compact space.

ASSUMPTION 3. The parameters  $\tau, \boldsymbol{\theta}, \sigma_\epsilon$  of the GP model are assumed known.

Recall  $\mathbf{x}_n = \arg \min g(\mathbf{x})$  and let  $\hat{\mathbf{x}}_N^*$  be the solution returned by the proposed algorithm when the simulation budget is  $N$ . The main theorem we are going to prove is as follows:

THEOREM 3. Suppose Assumptions 2–3 hold. Then as  $N$  tends to infinity, we have

$$g(\hat{\mathbf{x}}_N^*) - g(\mathbf{x}_n) \leq o_p(1), \quad (27)$$

i.e.,  $\hat{\mathbf{x}}_N^*$  nearly minimizes  $g(\mathbf{x})$ .

A natural corollary of the above theorem is that the sequence of points returned by Algorithm 1 converges to the global minimizer in probability if the set of optimum points includes only one element.

COROLLARY 1. Suppose Assumptions 2–3 hold. If the global optimal solution of  $g(x)$  is unique, then the following two results hold

$$\hat{\mathbf{x}}_N^* \rightarrow_p \mathbf{x}_n, \quad \text{as } N \rightarrow \infty.$$

When the number of real world data points  $n$  can also be increased to be infinity, we have the following result.

COROLLARY 2. Suppose conditions in Corollary 1 hold. Then for all  $\epsilon > 0$ , there exists  $n_0 > 0$  such that for all  $n' > n_0$ , there exists  $N'$  which depends on  $n'$ , such that  $\mathbb{P}(|\hat{\mathbf{x}}_N^* - \mathbf{x}^*| \geq \epsilon) < \epsilon$  and  $P(|g(\hat{\mathbf{x}}_N^*) - f(\mathbf{x}^*, \mathbf{P}^c)| \geq \epsilon) < \epsilon$  for any  $N \geq N'$ . In other words,

$$\hat{\mathbf{x}}_N^* \rightarrow_p \mathbf{x}^*, \quad \text{as } n, N \rightarrow \infty.$$

$$g(\hat{\mathbf{x}}_N^*) \rightarrow_p f(\mathbf{x}^*, \mathbf{P}^c), \quad \text{as } n, N \rightarrow \infty.$$

REMARK 4. Corollary 2 shows that, when both the size of the real world dataset  $n$  and the simulation budget  $N$  become large enough, the optimal solution/value returned from our algorithm can converge to the optimal solution/value of the true problem.

## 5. Numerical Experiments

### 5.1. An Inventory Example

In this section, we focus on the inventory problem of [Fu and Healy \(1997\)](#), which has been widely used to test the empirical performance of simulation optimization algorithms ([Jalali et al. 2017](#), [Wang et al. 2019a](#)). We will first test the empirical convergence of the optimal value/solution of the NBRO objective function to the optimal value/solution of the objective function under the true input distribution  $f(\mathbf{x}, \mathbf{P}^c)$ . We will then examine the empirical convergence of our proposed modified EGO algorithm in obtaining the optimal value/solution of the NBRO objective function. Lastly, we will compare the performance of our approach, which explicitly takes into account input uncertainty with approaches which overlook input uncertainty. This is to further highlight the importance of considering the NBRO problem when input uncertainty is high.

**5.1.1. Settings of the Inventory Simulator and Experiment** In the inventory problem of [Fu and Healy \(1997\)](#), a company manages the inventory of a single product with a periodic review policy. At the end of each period (e.g., each week), the company will check the inventory position with the following rule: if the inventory position is above the basic ordering level (denoted by  $s$ ), the company will not order; If the inventory position is below  $s$ , the company will order the difference between the order-up-to level (denoted by  $S$ ) and the inventory position. The decision variable  $\mathbf{x} = [s, S]$  is two dimensional. The customer demand, denoted by  $\xi$ , is stochastic and is independently identically distributed according to a distribution  $P$  across different periods. The cost includes the fixed ordering cost = 100, unit cost = 1, holding cost = 1, and backorder cost = 100. The candidate decision space is  $\{\mathbf{x} = [s, S] | s \in [10000, 22500], S \in [22600, 35000]\}$ . All these parameters used in this experiment are set to be the same as in [Jalali et al. \(2017\)](#). The simulator has been coded in Python, and has been validated by comparison with that of [Jalali et al. \(2017\)](#). The length of the simulation run was set to be 1000 periods with a warm-up length of 100 periods per simulation. The simulator output is the steady-state cost, which is the cost averaged over the 900 (= 1000 – 100) periods. For a given decision  $\mathbf{x}$  and a given demand distribution  $P$ , each simulation run produces an output  $y(\mathbf{x}, P) = h(\mathbf{x}, \xi), \xi \sim P$ . The expected steady-state cost (expected simulation output) for a given decision  $\mathbf{x}$  and a given demand distribution  $P$  is denoted by  $f(\mathbf{x}, P)$ .

We assume the true distribution of the demand  $P^c$  to be  $\exp(\lambda^c)$ , where  $\lambda^c = 0.0002$  is the true value of the input parameter. The true expected steady-state cost function is denoted by  $f(\mathbf{x}, P^c)$ . Ideally, we aim to solve the problem of  $\min_{\mathbf{x}} f(\mathbf{x}, P^c)$ . When the true demand distribution  $P^c$  is exponential, there is a closed form expression for the expected cost function, and the optimal decision can be calculated analytically. The expected cost function is given by

$$f(\mathbf{x}, P^c = \exp(\lambda^c)) = \frac{1}{100} \left[ \frac{1}{\lambda^c} + \left[ 100 + s - \frac{1}{\lambda^c} + 0.5\lambda^c(S^2 - s^2) + \frac{101}{\lambda^c} e^{-\lambda^c s} \right] / [1 + \lambda^c(S - s)] \right]. \quad (28)$$

In practice, however, the true input distribution  $P^c$  is unknown (i.e., both the exponential distribution and the value of  $\lambda^c$  are unknown). Instead, only a finite set of real data  $\mathbf{D}_n = \{\xi_1, \dots, \xi_n\}$ , where  $\xi_i \sim P^c, i = 1, \dots, n$  can be observed. Therefore, we cannot use the analytical expression in (28) to calculate the optimal decision  $\mathbf{x}^* = \arg \min_{\mathbf{x}} f(\mathbf{x}, P^c)$  directly. What is available is the simulator, from which the simulation output  $y(\mathbf{x}, P)$  can be obtained for a given decision  $\mathbf{x}$  and a given demand distribution  $P$ .

Under the NBRO approach, we model  $P^c$  as a random variable  $P$ . We assume a Dirichlet prior for  $P$  with  $\alpha = 1$  and  $P_0 = \text{uniform}(0, \max(\xi_1, \dots, \xi_n))$  (as recommended in (Gelman et al. 2013)). Then we solve the problem of  $\min_{\mathbf{x}} g(\mathbf{x}) = \mathbb{E}_{P \sim \pi} [f(\mathbf{x}, P)]$ . As the exact form of  $f(\mathbf{x}, P)$  and  $g(\mathbf{x})$  is unknown, our proposed GP algorithm first builds a GP model  $F_s(\mathbf{x}, P)$  for  $f(\mathbf{x}, P)$  and then constructs a GP model  $\hat{G}_s(\mathbf{x})$  for  $g(\mathbf{x})$ . Both  $F_s(\mathbf{x}, P)$  and  $\hat{G}_s(\mathbf{x})$  are updated sequentially as additional points are selected to be evaluated by our proposed EGO algorithm. When the total budget is exhausted, the optimal solution is returned based on  $\mu_N(\mathbf{x})$ , the predictive mean for  $g(\mathbf{x})$ , as follows:  $\hat{\mathbf{x}}^* = \arg \min_{\mathbf{x} \in \mathcal{V}_N} \mu_N(\mathbf{x})$ .

**5.1.2. Empirical Convergence and Asymptotic Normality of the NBRO** Theoretical convergence properties of the NBRO are provided in Section 3. Here, we aim to illustrate the empirical convergence of the optimal value/solution of the NBRO to the optimal value/solution of the  $f(\mathbf{x}, P^c)$  for finite  $n$ . We consider two evaluation metrics,  $|f(\mathbf{x}^*, P^c) - \min g(\mathbf{x})|$  and  $\|\mathbf{x}^* - \arg \min g(\mathbf{x})\|$ . As  $g(\mathbf{x})$  is not directly observable, we approximate it by  $\frac{1}{10000} \sum_{i=1}^{10000} \bar{y}(\mathbf{x}, P_i)$ , where  $\bar{y}(\mathbf{x}, P_i)$  is the average of 1000 simulation outputs at  $(\mathbf{x}, P_i)$ , and we use a grid search over a large set of the design points to obtain  $\min_{\mathbf{x}} g(\mathbf{x})$  and  $\arg \min_{\mathbf{x}} g(\mathbf{x})$ . We consider nine cases of the number  $n$  of real world data points, with  $n$  set at 10, 20, 50, 100, 500, 1000, 10000, 100000 and 500000. We conducted 100 replications and calculated the mean values of the  $|f(\mathbf{x}^*, P^c) - \min g(\mathbf{x})|$  and

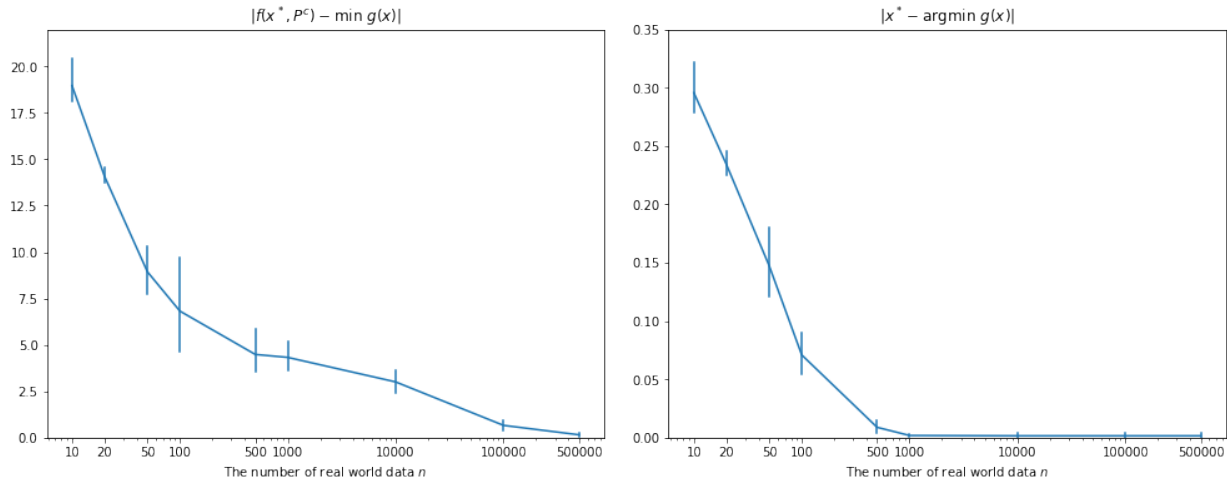


**Figure 2** Empirical convergence of the NBRO optimal value to the true optimal value

**Figure 3** Empirical convergence of the NBRO optimal solution to the true optimal solution

$\|\mathbf{x}^* - \text{argmin } g(\mathbf{x})\|$  and their 95% confidence intervals over the 100 replications. The results are shown in Figure 2 and Figure 3. The two figures show that the optimal value/solution of the NBRO will approach to the optimal value/solution of  $f(\mathbf{x}, P^c)$  as  $n$  becomes large.

In addition, the Jarque–Bera normality test (Jarque and Bera 1980) on the values of  $\sqrt{n}(f(\mathbf{x}^*, P^c) - \min g(\mathbf{x}))$  and Mardia’s multivariate normality test (Mardia 1980) on the values of  $\sqrt{n}(\mathbf{x}^* - \text{argmin } g(\mathbf{x}))$  over the 100 replications tests both confirm normality for  $n = 500000$ , which helps validate Theorem 2 (ii) and (iii).

**5.1.3. Empirical Convergence of the Proposed Algorithm** In this section, we test the efficiency of our proposed algorithm in solving the NBRO problem given by (8). We define  $\text{gGAP} = |\min_{\mathbf{x}} g(\mathbf{x}) - g(\hat{\mathbf{x}}^*)|$  and  $\text{gxGAP} = \|\text{argmin}_{\mathbf{x}} g(\mathbf{x}) - \hat{\mathbf{x}}^*\|$ . These are used to test whether the returned value/solution of our proposed GP algorithm is able to converge to the optimal value/solution of  $g(\mathbf{x})$ .

We follow the suggestion of Jones et al. (1998) to take the initial size of the design sample to be  $10 \times d = 30$ , where  $d = 3$  is the dimension of the function, and sequentially select an additional 100 points to be evaluated. For evaluation at each point  $(\mathbf{x}, P)$ , we use  $r = 10$  replications to determine the value of  $\bar{y}(\mathbf{x}, P)$ . Therefore, the total budget is  $(30 + 100) \times 10 = 1300$ . We conducted 100 macro-replications and calculated the means of both gGAP and gxGAP and their 95% confidence intervals. We set  $n = 10$ . The results are shown in Figure 4 and Figure 5. The two figures show that as the number of iterations (budget) increases, the optimal value/solution returned by our algorithm is able to get

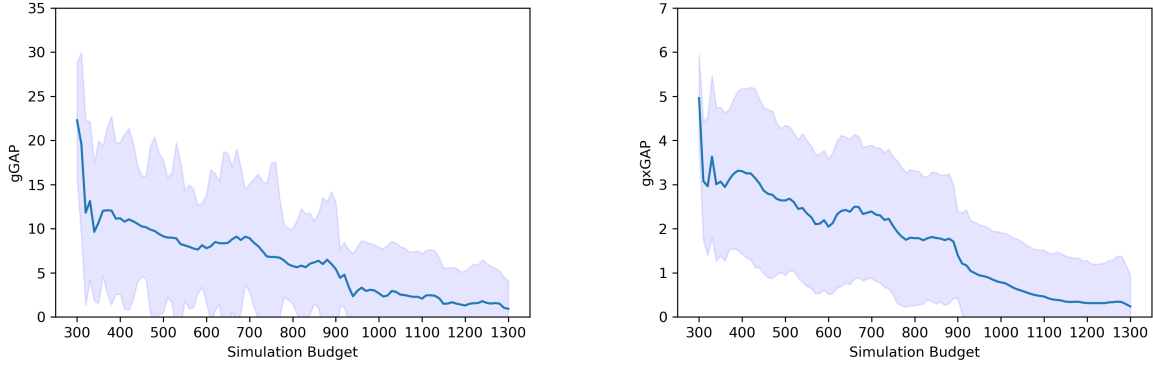


**Figure 4** Empirical performance in terms of gGAP of our GP based algorithm with respect to the size of the budget.

**Figure 5** Empirical performance in terms of gxGAP of our GP based algorithm with respect to the size of the budget.

close to the optimal value/solution of the  $g(\mathbf{x})$ . We observe similar convergence trends when  $n$  increases to 1000.

**5.1.4. Comparison of the NBRO with existing approaches** In this section, we aim to compare the NBRO approach with some other approaches for solving problem (1) when the true input distribution  $P^c$  is unknown.

As was mentioned in Section 1, when the true input distribution  $P^c$  is unknown, it is common in practice to ignore the input uncertainty and directly use an estimated input distribution  $\hat{P}$  as if it were the true input distribution. This approach then solves (2), ignoring the input uncertainty. We refer to this approach as the Plug-In (PI) approach. The empirical cumulative distribution computed from the real data,  $\hat{P}(t) = \frac{1}{n} \sum_{i=1}^n 1_{\xi_i \leq t}$ , is usually chosen as the estimated input distribution. The PI approach can be solved using sequential kriging optimization (SKO), a variant of the EGO algorithm, proposed by Huang et al. (2006), in which a GP model is built for  $f(\mathbf{x}, \hat{P})$  with predictive mean denoted by  $\hat{f}(\mathbf{x}, \hat{P})$ . The obtained optimizer is given by  $\hat{\mathbf{x}}^* = \arg \min_{\mathbf{x} \in \mathcal{V}'_N} \hat{f}(\mathbf{x}, \hat{P})$ , where  $\mathcal{V}'_N$  is the set of all evaluated design points. In addition, modeling the input uncertainty from a parametric Bayesian perspective is also widely used (Xie et al. 2014, Wu et al. 2018, Wang et al. 2019a). Specifically, it is assumed that the true input distribution  $P^c$  belongs to some parametric family of distributions, with an unknown input parameter  $\lambda_c$ . Similar to the NBRO, we consider the risk-neutral case. The objective function is  $\min_{\mathbf{x} \in \mathcal{X}} \mathbb{E}_{\lambda \sim \pi} [\mathbb{E}_{\xi \sim P_\lambda} [h(\mathbf{x}, \xi)]]$ . The equation can be solved with an modified EGO algorithm combined with the integrated mean squared error criterion proposed in Wang et al. (2019a).



Here, we will refer to this approach as the parametric Bayesian (PB) approach. For the parametric Bayesian approach, we consider two cases. One is that the parametric family of the input distribution is correctly selected, i.e., the exponential distribution (denoting this case as “PB exponential”). Another is that the parametric family is wrongly selected to be log-normal (denoting this case as “PB log-normal”). Here, we aim to investigate the effect of the choice of the parametric family on the performance. For “PB exponential,” the random demand  $\xi_i$  is assumed to follow  $\exp(\lambda)$  with the parameter  $\lambda$ . A non-informative Jeffreys prior  $p(\lambda) \propto 1/\lambda$  is posed on  $\lambda$  and the posterior distribution is the Gamma distribution. For “PB log-normal,” the natural logarithm of the random demand  $\ln(\xi_i)$  is assumed to follow the normal distribution  $N(\mu, \sigma^2)$  with parameter  $\mu$  and  $\sigma^2$ . We assume a non-informative Jeffreys prior  $p(\mu, \sigma^2) \propto 1/\sigma^2$  for the two parameters: then the posterior distribution is the Normal-Inverse-Gamma distribution.

We define  $\text{GAP} = |f(\mathbf{x}^*, P^c) - f(\hat{\mathbf{x}}^*, P^c)|$ : it measures directly the loss incurred from the estimated minimizer  $\hat{\mathbf{x}}^*$ . We use also 100 macro-replications with different initial Latin Hypercube design points for each macro-replication. For a given macro-replication, the four approaches start with the same initial design points. Twenty points are selected sequentially after the initial design. Therefore, the total budget is  $(30 + 20) \times 10 = 500$ . Here we consider the performance of these approaches under different levels of input uncertainty, which can be roughly controlled by the size  $n$  of the real world dataset. We consider four cases of this number  $n$ : 10, 50, 100, and 1000. The results of the comparison are summarized and shown in the box plots in Figure 6. We use Mood’s median test (Mood 1954) with a significance level of 0.05 to test whether there are significant differences between the medians of the GAP of the different approaches.

We first compare the performance of NBRO and PI in order to see the potential benefits of NBRO. Mood’s median test shows that the difference is not significant when  $n$  is 1000. When  $n$  is 10, 50, or 100, the differences are significant. When  $n$  is equal to 1000, the GAP performances for both approaches tend to be zero, and the variance of this measure is small. This result can be expected because as  $n$  increases, the level of the input uncertainty will decrease. When  $n$  tends to infinity (i.e., the input uncertainty vanishes), both the posterior  $\boldsymbol{\pi}(P|\mathbf{D}_n)$  and the empirical cumulative distributions  $\hat{P}$  will be similar to the true input distribution  $P^c$ . As a result, both the NBRO and the PI approaches will reduce to the true problem (1), and hence it is expected that the minimizers from both approaches

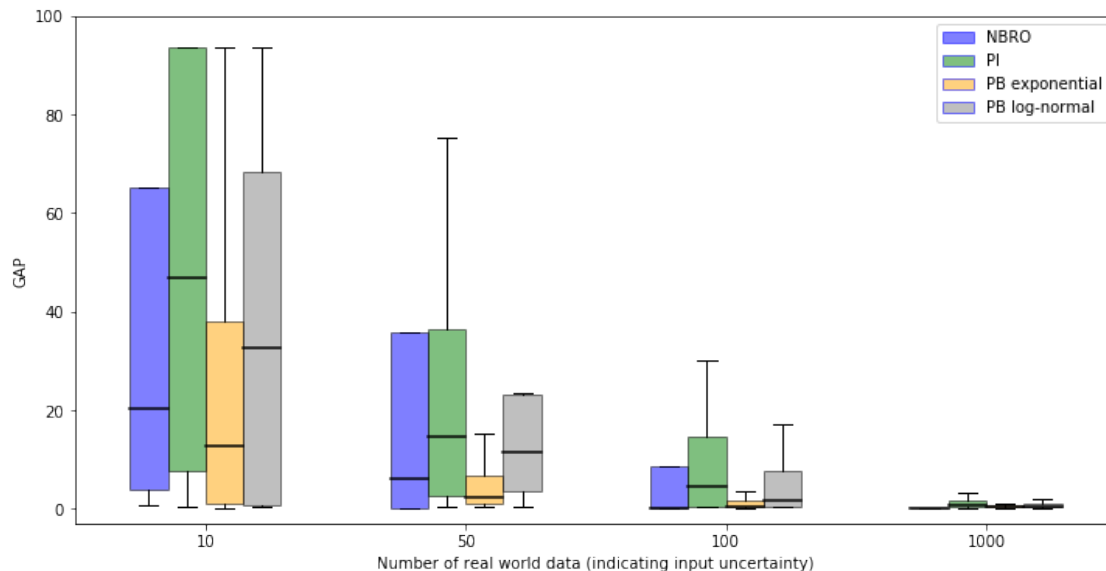


**Figure 6** Boxplot of the GAP values for the approaches (NBRO, PI, Bayesian Parametric (exponential) and Bayesian Parametric (gamma)) under different levels of input uncertainty. The black solid lines within the boxes represent the medians.

converge. However, when  $n = 10$  and  $n = 50$ , the performance of the NBRO approach is significantly better than that of the PI approach. When  $n = 100$ , the proposed NBRO approach achieves both a smaller median and variance than its counterpart. Although for this amount of data the median of the PI approach is not very large, its variance is large, indicating that this approach is highly dependent on the estimated empirical distribution  $\hat{P}$ . This result is consistent with our motivation for proposing NBRO (as highlighted in Section 1). It also can be noted that when  $n$  becomes large, like  $n = 1000$  and with a reasonably finite number of the simulation evaluations, like 500 in this example, the GAP values of the NBRO become very close to 0 with very small variance, which indicates that the estimated solution approaches to the true solution.

Now we compare the performance of the NBRO and the parametric Bayesian approach with both correct and wrong families of parametric distributions. When the level of input uncertainty is high, i.e.,  $n = 10$  or  $n = 50$ , “PB exponential” is better than NBRO. This result is reasonable, as the Bayesian Parametric approach requires more information assuming that the exponential distribution family is known. In contrast, the performance of “PB log-normal” is worse than that of NBRO, which shows the risk of choosing the wrong family of distributions for the input distribution in simulation optimization.

The good performance of our proposed algorithm comes at a cost of longer computational times. The total time required to run the whole algorithm (30 initial design points and additional 20 evaluation points with 10 simulation replications in each point for  $n = 10$ ) was 135.4, 25.3, 27.1 minutes for our method, PI and PB respectively. Although the computational time for our proposed approach is higher than that of the plug-in and unknown parameter methods, the differences are not too large and are reasonable for decisions required for longer periods. This also suggests that our method is well suited for expensive simulations (common in practice), where the evaluation time on the simulation model is much longer than the time required for selecting the subsequent evaluation point.

In summary, the proposed NBRO approach with the modified EGO algorithm which explicitly considers input uncertainty is more robust to the level of input uncertainty compared with the PI approach, which ignores it. This further illustrates that our approach can be effective in hedging the risk that arises from input uncertainty in simulation optimization, especially when this uncertainty is high. For the parametric approaches, it is clear that using the approaches which assume more information about the distribution family can sometimes bring about additional risks when the assumption involves errors. The additional risks can lead to sub-optimal or even wrong decisions. The proposed NBRO that requires no information as to the family of distributions is more robust.

## 5.2. Critical Care Facility

In this section, we use the critical care facility system which has been studied in [Ng and Chick \(2006\)](#) and [Xie et al. \(2014\)](#) to illustrate the performance of our algorithm.

The simulation output of the system is the steady-state number of patients denied a bed per day. Patients arriving at the facility will be allocated, depending on their health condition, to either the intensive care unit (ICU) or the coronary care unit (CCU), and then exit the facility or go to the intermediate ICU (IICU) or the intermediate CCU (ICCU). The IICU and the ICCU share the beds in the Intermediate Care (IC). Arriving patients who cannot get a bed in ICU or CCU will be denied entry. If one patient is supposed to move to the IC but there is no bed available in the IC, he/she will stay put (in ICU/CCU) and queue for a bed in the IC. When a bed in the IC becomes available, the first patient in the queue will be transferred. Figure 7 depicts the system.

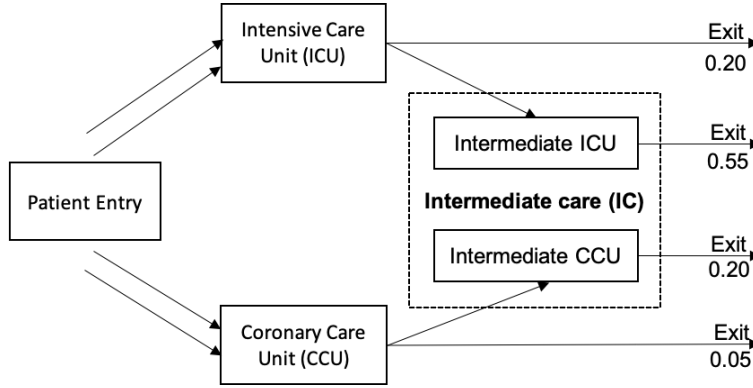


**Figure 7** Critical care facility

There are three design variables in the system: the number of beds in the ICU, the CCU and the IC, denoted by  $\mathbf{x} = [x_1, x_2, x_3]^T$ . It can be expected that, the larger the number of the beds in the three units, the lower the expected number of patient will be denied entry per day. However, the resources in the facility will be always limited. The difficulty is to balance the number of the beds of the three different units under limited resources. The costs of holding an IC bed is usually half of that of the ICU and CCU, as less staff are needed per patient in the IC (Plate et al. 2017). Therefore, we consider the design space to be  $\mathcal{X} = \{\mathbf{x} = [x_1, x_2, x_3] | 26 \leq x_1 + x_2 + 0.5x_3 \leq 28, x_1 \in N_+, x_2 \in N_+, x_3 \in N_+\}$ . The total number of candidate design points is 1273.

The system also includes six input processes: the interarrival time of patients, the stay duration in ICU, CCU, IICU and ICCU, and the routing of patients. The setting for the true input distribution, denoted by  $\mathbf{P}^c = [P^{c(1)}, P^{c(2)}, P^{c(3)}, P^{c(4)}, P^{c(5)}, P^{c(6)}]$ , is as follows. The interarrival time of patients ( $P^{c(1)}$ ) is exponentially distributed with rate being 3.3/day, i.e. patients are arriving according to a Poisson process. The stay duration is lognormal-distributed in the four units: the mean values of the stay duration in ICU, CCU, IICU and ICCU ( $P^{c(2)}, P^{c(3)}, P^{c(4)}$  and  $P^{c(5)}$ ) are 3.4, 3.8, 15.0 and 17.0 days respectively, and the values of the standard deviation of the stay duration are 3.5, 1.6, 7.0 and 3.0 days respectively. The routing of the each patient ( $P^{c(6)}$ ) follows a discrete distribution with probability 0.2, 0.55, 0.2 and 0.05.

Each simulation starts with an empty system. We set the run length for each simulation to be 300 days beyond a warm-up period of 300 days, which is discarded to avoid bias. To evaluate our method, we assume that the input distributions of the six input processes are unknown and are estimated from  $n = 1000$  independent and identically distributed random

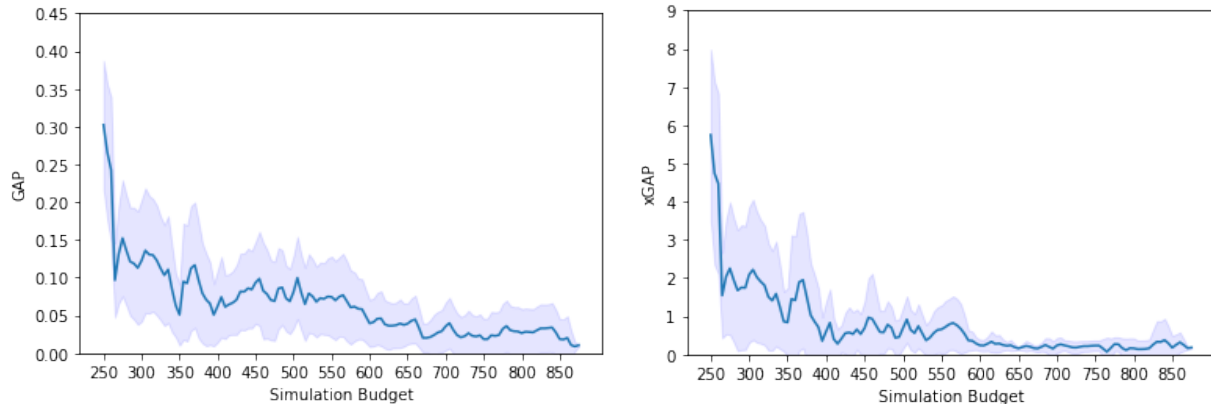


**Figure 8** GAP for the critical care facility problem    **Figure 9** xGAP for the critical care facility problem

variables from each of the six true input distributions. Denote the input distribution by  $\mathbf{P} = [P^{(1)}, P^{(2)}, P^{(3)}, P^{(4)}, P^{(5)}, P^{(6)}]$ . 50 initial design points are used to construct the GP with 5 replications at each point, and additional 125 points are selected from our algorithm. The total simulation budget is then  $(50 + 125) \times 5 = 875$ . As  $f(x, P^c)$  is unknown for this complex system, we instead use a long enough run lengths of  $10^4$  days (as recommended in Xie et al. (2014)) to estimate the system mean response, and then estimate the optimal solution  $\mathbf{x}^* = \arg \min_{\mathbf{x}} f(\mathbf{x}, P^c)$  and optimal value  $f(\mathbf{x}^*, P^c)$  based on the estimated mean response. The estimated true optimal solution  $\mathbf{x}^*$  is  $[12, 5, 22]$  and the estimated optimal value  $f(\mathbf{x}^*, P^c)$  is 0.596.

We consider two evaluation metric:  $\text{GAP} = |f(\mathbf{x}^*, P^c) - f(\hat{\mathbf{x}}^*, P^c)|$  and  $\text{xGAP} = \|\mathbf{x}^* - \hat{\mathbf{x}}^*\|$ . The results are shown in Figure 8 and Figure 9. It shows that the optimal value and optimal solution returned from our algorithm will empirically converge (with a reasonably finite  $n$  and  $N$ ) to the true optimal value and true optimal solution. The theoretical convergence properties have already been provided in Corollary 2.

## 6. Conclusion

In this paper, we considered the stochastic simulation optimization problem when the input distribution is unknown. We first formulated the nonparametric Bayesian risk optimization (NBRO) problem and proposed using a nonparametric Bayesian approach to model the input uncertainty. We studied the asymptotic consistency and normality of the NBRO to ensure its theoretical performance. Then the Efficient Global Optimization (EGO) algorithm was extended to solve this NBRO problem. We studied the consistency properties

of the modified EGO algorithm and tested its efficiency empirically with an inventory example and a critical care facility problem. From the results of the numerical experiment, we find that: 1) The optimal solution and optimal value of the NBRO will get close to the optimal solution and optimal value of  $f(\mathbf{x}, \mathbf{P}^c)$  as the amount of real world data becomes large (input uncertainty level decreases). 2) Our proposed algorithm can empirically converge to the optimal value and solution of the NBRO objective function  $g(\mathbf{x})$ . This essentially shows that our proposed algorithm, which uses a fast approximation, can locate the global minimizer of the NBRO problem accurately, and can be applied to efficiently solve the NBRO problem; 3) Compared with approaches that ignores the input uncertainty, our algorithm is able to obtain solutions closer to the optimal value of  $f(\mathbf{x}, \mathbf{P}^c)$ . In addition, the NBRO approach can avoid the risk of choosing a wrong parametric family in the parametric Bayesian approach. The NBRO appears to be more robust to the level of input uncertainty, which illustrates the benefits of considering the NBRO as the objective in stochastic simulation optimization when input uncertainty is present.

There are several directions for future work. First, in this paper, we focus on the expectation risk function which is risk neutral. It would be interesting to explore other risk functions such as mean-variance, Value at Risk and Conditional Value at Risk. Second, as noted in the paper, other GP-based optimization algorithms, such as Knowledge Gradient, can also be adjusted for input uncertainty. The performance of other algorithms can be further investigated. Finally, it is possible to reduce the computational time for our method by parallel computing, faster Monte Carlo sampling methods (Rubinstein and Kroese 2016) and more efficient computation algorithms of Wasserstein distances (Chizat et al. 2020), which we leave for future research.

## Acknowledgments

This work was supported in part by the Ministry of Education, Singapore (Grant R-266-000-149-114).

## References

- Ankenman B, Nelson BL, Staum J (2010) Stochastic kriging for simulation metamodeling. *Operations Research* 58(2):371–382.
- Ankenman BE, Nelson BL (2012) A quick assessment of input uncertainty. *Proceedings of the 2012 Winter Simulation Conference (WSC)*, 1–10 (IEEE).
- Bachoc F, Gamboa F, Loubes JM, Venet N (2017) A Gaussian process regression model for distribution inputs. *IEEE Transactions on Information Theory* 64(10):6620–6637.

- Barcella W, De Iorio M, Favaro S, Rosner GL (2018) Dependent generalized dirichlet process priors for the analysis of acute lymphoblastic leukemia. *Biostatistics* 19(3):342–358.
- Barton RR, Meckesheimer M (2006) Metamodel-based simulation optimization. *Handbooks in Operations Research and Management Science* 13:535–574.
- Barton RR, Schruben LW (1993) Uniform and bootstrap resampling of empirical distributions. *Proceedings of the 25th Conference on Winter Simulation*, 503–508 (ACM).
- Barton RR, Schruben LW (2001) Resampling methods for input modeling. *Proceedings of the 33rd Conference on Winter Simulation*, 372–378 (IEEE Computer Society).
- Chick SE (2001) Input distribution selection for simulation experiments: Accounting for input uncertainty. *Operations Research* 49(5):744–758.
- Chizat L, Roussillon P, Léger F, Vialard FX, Peyré G (2020) Faster wasserstein distance estimation with the sinkhorn divergence. *arXiv preprint arXiv:2006.08172* .
- Christensen R, Johnson W (1988) Modelling accelerated failure time with a dirichlet process. *Biometrika* 75(4):693–704.
- Cressie N (1992) Statistics for spatial data. *Terra Nova* 4(5):613–617.
- De Oliveira V, Kone B (2015) Prediction intervals for integrals of Gaussian random fields. *Computational Statistics and Data Analysis* 83:37–51.
- Fan Q, Hu J (2018) Surrogate-based promising area search for lipschitz continuous simulation optimization. *INFORMS Journal on Computing* 30(4):677–693.
- Ferguson TS (1973) A Bayesian analysis of some nonparametric problems. *The Annals of Statistics* 209–230.
- Frazier P, Powell W, Dayanik S (2009) The knowledge-gradient policy for correlated normal beliefs. *INFORMS Journal on Computing* 21(4):599–613.
- Frazier PI (2018) Bayesian optimization. *Recent Advances in Optimization and Modeling of Contemporary Problems*, 255–278 (INFORMS).
- Fu MC, Healy KJ (1997) Techniques for optimization via simulation: An experimental study on an (s, s) inventory system. *IIE Transactions* 29(3):191–199.
- Fuglede B, Topsoe F (2004) Jensen-shannon divergence and hilbert space embedding. *International Symposium on Information Theory, 2004. ISIT 2004. Proceedings.*, 31 (IEEE).
- Gelman A, Stern HS, Carlin JB, Dunson DB, Vehtari A, Rubin DB (2013) *Bayesian Data Analysis* (Chapman and Hall/CRC).
- Ghosh S, Lam H (2019) Robust analysis in stochastic simulation: Computation and performance guarantees. *Operations Research* 67(1):232–249.
- Heath TA, Holder MT, Huelsenbeck JP (2012) A dirichlet process prior for estimating lineage-specific substitution rates. *Molecular biology and evolution* 29(3):939–955.

- Hein M, Bousquet O (2004) Hilbertian metrics and positive definite kernels on probability measures .
- Hjort NL, Holmes C, Müller P, Walker SG (2010) *Bayesian Nonparametrics*, volume 28 (Cambridge University Press).
- Huang D, Allen TT, Notz WI, Zeng N (2006) Global optimization of stochastic black-box systems via sequential kriging meta-models. *Journal of Global Optimization* 34(3):441–466.
- Jalali H, Van Nieuwenhuyse I, Picheny V (2017) Comparison of kriging-based algorithms for simulation optimization with heterogeneous noise. *European Journal of Operational Research* 261(1):279–301.
- Jarque CM, Bera AK (1980) Efficient tests for normality, homoscedasticity and serial independence of regression residuals. *Economics letters* 6(3):255–259.
- Jones DR, Schonlau M, Welch WJ (1998) Efficient global optimization of expensive black-box functions. *Journal of Global Optimization* 13(4):455–492.
- Kushner H, Yin G (2003) *Stochastic Approximation and Recursive Algorithms and Applications* (Springer-Verlag New York).
- Lam H (2016) Advanced tutorial: Input uncertainty and robust analysis in stochastic simulation. *Proceedings of the 2016 Winter Simulation Conference*, 178–192 (IEEE Press).
- Locatelli M (1997) Bayesian algorithms for one-dimensional global optimization. *Journal of Global Optimization* 10(1):57–76.
- Mardia KV (1980) 9 tests of univariate and multivariate normality. *Handbook of statistics* 1:279–320.
- Mood AM (1954) On the asymptotic efficiency of certain nonparametric two-sample tests. *The Annals of Mathematical Statistics* 514–522.
- Ng SH, Chick SE (2006) Reducing parameter uncertainty for stochastic systems. *ACM Transactions on Modeling and Computer Simulation (TOMACS)* 16(1):26–51.
- Ng SH, Yin J (2012) Bayesian kriging analysis and design for stochastic simulations. *ACM Transactions on Modeling and Computer Simulation (TOMACS)* 22(3):17.
- Ólafsson S (2006) Metaheuristics. *Handbooks in Operations Research and Management Science* 13:633–654.
- Pearce M, Branke J (2017) Bayesian simulation optimization with input uncertainty. *Proceedings of the 2017 Winter Simulation Conference*, 181 (IEEE Press).
- Pedrielli G, Wang S, Ng SH (2020) An extended two-stage sequential optimization approach: Properties and performance. *European Journal of Operational Research* .
- Peyré G, Cuturi M, et al. (2019) Computational optimal transport. *Foundations and Trends® in Machine Learning* 11(5-6):355–607.
- Picheny V (2015) Multiobjective optimization using Gaussian process emulators via stepwise uncertainty reduction. *Statistics and Computing* 25(6):1265–1280, ISSN 15731375.



- Plate JD, Leenen LP, Houwert M, Hietbrink F (2017) Utilisation of intermediate care units: a systematic review. *Critical care research and practice* 2017.
- Rasmussen CE (2004) Gaussian processes in machine learning. *Advanced Lectures on Machine Learning*, 63–71 (Springer).
- Rubinstein RY, Kroese DP (2016) *Simulation and the Monte Carlo method*, volume 10 (John Wiley & Sons).
- Song E, Nelson BL (2015) Quickly assessing contributions to input uncertainty. *IIE Transactions* 47(9):893–909.
- Song E, Nelson BL, Pegden CD (2014) Advanced tutorial: Input uncertainty quantification. *2014 Simulation Conference (WSC)*, 162–176 (IEEE).
- Stuart AM, Teckentrup AL (2018) Posterior consistency for Gaussian process approximations of Bayesian posterior distributions. *Mathematics of Computation of the American Mathematical Society* 87(310):721–753.
- Van der Vaart AW (2000) *Asymptotic statistics*, volume 3 (Cambridge university press).
- Villemonteix J, Vazquez E, Walter E (2009) An informational approach to the global optimization of expensive-to-evaluate functions. *Journal of Global Optimization* 44(4):509.
- Wang H, Yuan J, Ng SH (2019a) Gaussian process based optimization algorithms with input uncertainty. *IIE Transactions* 52(4):37–393.
- Wang S, Ng SH, Haskell WB (2019b) A multi-level simulation optimization approach for quantile functions. *arXiv preprint arXiv:1901.05768* .
- Wu D, Zhu H, Zhou E (2018) A Bayesian risk approach to data-driven stochastic optimization: Formulations and asymptotics. *SIAM Journal on Optimization* 28(2):1588–1612.
- Xie W, Li C, Wu Y, Zhang P (2019) A Bayesian nonparametric framework for uncertainty quantification in simulation. *arXiv preprint arXiv:1910.03766* .
- Xie W, Nelson BL, Barton RR (2014) A Bayesian framework for quantifying uncertainty in stochastic simulation. *Operations Research* 62(6):1439–1452.
- Xu J, Huang E, Chen CH, Lee LH (2015) Simulation optimization: A review and exploration in the new era of cloud computing and big data. *Asia-Pacific Journal of Operational Research* 32(03):1550019.
- Zhou E, Xie W (2015) Simulation optimization when facing input uncertainty. *Proceedings of the 2015 Winter Simulation Conference*, 3714–3724 (IEEE Press).
- Zouaoui F, Wilson JR (2003) Accounting for parameter uncertainty in simulation input modeling. *IIE Transactions* 35(9):781–792.

## Proofs of Statements

### EC.1. Formulate the objective function as i.i.d summation

*Proof of Lemma 1* Recall that  $\xi_1, \dots, \xi_n \sim P^c$ . We model  $P^c$  with a prior  $P \sim DP(\alpha, P_0)$ , where  $DP(\alpha, P_0)$  is a Dirichlet process parametrized by the parameter  $\alpha$  and the base distribution  $P_0$ . Denote the posterior distribution by  $\pi(P|\xi_1, \dots, \xi_n)$ . Then we have  $\pi(P|\xi_1, \dots, \xi_n) \sim DP(\alpha + n, \frac{\alpha P_0 + \sum_{j=1}^n \delta_{\xi_j}}{\alpha + n})$ . Without loss of generality, we can assume  $\bar{\xi}_i - \underline{\xi}_i = \delta_i$  for all  $i = 1, 2, \dots, l$ . For a fixed  $m$ , considering the following partition

$$\begin{aligned} [\underline{\xi}_i, \bar{\xi}_i] &= [\underline{\xi}_i, \underline{\xi}_i + \frac{\delta_i}{m}] \cup (\underline{\xi}_i + \frac{\delta_i}{m}, \underline{\xi}_i + \frac{2\delta_i}{m}] \cup \dots \cup (\bar{\xi}_i - \frac{\delta_i}{m}, \bar{\xi}_i] = \cup_{k=1}^m B_k^{(i)} \\ \Omega &= \cup_{k_1, k_2, \dots, k_l} B_{k_1}^{(1)} \times B_{k_2}^{(2)} \times \dots \times B_{k_l}^{(l)}, \quad k_i = 1, 2, \dots, m, \text{ for } i = 1, \dots, l \\ &= \cup_{i=1}^{m^l} A_i (A_i = B_{k_1}^{(1)} \times B_{k_2}^{(2)} \times \dots \times B_{k_l}^{(l)}). \end{aligned}$$

Now, denote the center of  $A_i$  by  $\mathbf{c}_i$  and consider the piece-wise constant function

$$h_m(\mathbf{x}, \xi) = \begin{cases} h(\mathbf{x}, \mathbf{c}_1), & \xi \in A_1 \\ h(\mathbf{x}, \mathbf{c}_2), & \xi \in A_2 \\ \dots \\ h(\mathbf{x}, \mathbf{c}_{m^l}), & \xi \in A_{m^l}. \end{cases}$$

For any distribution  $P$ , we have

$$\mathbb{E}_{\xi \sim P}[h(\mathbf{x}, \xi)] = \lim_{m \rightarrow +\infty} \sum_{i=1}^{m^l} h(\mathbf{x}, \mathbf{c}_i) P(A_i) = \lim_{m \rightarrow +\infty} \mathbb{E}_{\xi \sim P}[h_m(\mathbf{x}, \xi)]$$

Since  $h(\mathbf{x}, \xi)$  is Lipschitz, we know  $\sup_{\xi} |h_m(\mathbf{x}, \xi) - h(\mathbf{x}, \xi)| \leq \frac{L_1 \delta}{m}$ , where  $\delta = \sqrt{\delta_1^2 + \delta_2^2 + \dots + \delta_l^2}$ , so

$$\left| \sum_{i=1}^{m^l} h(\mathbf{x}, \mathbf{c}_i) P(A_i) - \mathbb{E}_P[h(\mathbf{x}, \xi)] \right| = |\mathbb{E}_P[h_m(\mathbf{x}, \xi)] - \mathbb{E}_P[h(\mathbf{x}, \xi)]| \leq \frac{L_1 \delta}{m}$$

As a result, if we put  $Q_m(P) = \sum_{i=1}^{m^l} h(\mathbf{x}, \mathbf{c}_i) P(A_i)$ , then  $Q_m(P) \rightarrow \mathbb{E}_P[h(\mathbf{x}, \xi)]$  uniformly in  $P$ . We now compute

$$\mathbb{E}_{\pi}[\mathbb{E}_P[h(\mathbf{x}, \xi)]] = \mathbb{E}_{\pi} \left[ \lim_m Q_m(P) \right] = \lim_m \mathbb{E}_{\pi}[Q_m(P)]. \quad (\text{EC.1})$$

We can exchange the order of limit and expectation in (EC.1) because  $Q_m(\mathbf{P}) \rightarrow \mathbb{E}_{\mathbf{P}}[h(\mathbf{x}, \boldsymbol{\xi})]$  uniformly in  $\mathbf{P}$ . For any fixed  $m$ , we can compute

$$\begin{aligned} \mathbb{E}_{\pi}[Q_m(\mathbf{P})] &= \sum_{i=1}^m h(\mathbf{x}, \mathbf{c}_i) \mathbb{E}_{\pi}(\mathbf{P}(A_i)) \\ &= \sum_{i=1}^m h(\mathbf{x}, \mathbf{c}_i) \left( \frac{\alpha \mathbf{P}_0(A_i)}{\alpha + n} + \frac{1}{\alpha + n} \sum_{j=1}^n \delta_{\boldsymbol{\xi}_j}(A_i) \right) \end{aligned}$$

The first term of the above equation converges to  $\mathbb{E}_{\mathbf{P}_0} \frac{\alpha}{\alpha+n} h(\mathbf{x}, \boldsymbol{\xi})$  by definition. We now consider the second term. For fixed  $n$ , when  $m$  tends to infinity,

$$\begin{aligned} &\lim_{m \rightarrow +\infty} \sum_{i=1}^m \left( h(\mathbf{x}, \mathbf{c}_i) \times \frac{1}{\alpha + n} \sum_{j=1}^n \delta_{\boldsymbol{\xi}_j}(A_i) \right) \\ &= \frac{1}{\alpha + n} \sum_{j=1}^n \lim_{m \rightarrow +\infty} \sum_{i=1}^m h(\mathbf{x}, \mathbf{c}_i) \delta_{\boldsymbol{\xi}_j}(A_i) \\ &= \frac{1}{\alpha + n} \sum_{j=1}^n \lim_{m \rightarrow +\infty} h(\mathbf{x}, \mathbf{c}_{i'}) \text{ (such that } \boldsymbol{\xi}_j \in A_{i'}, i' \in 1, \dots, m^l) \\ &= \frac{1}{\alpha + n} \sum_{j=1}^n h(\mathbf{x}, \boldsymbol{\xi}_j). \end{aligned}$$

The second equality holds because the partitions  $A_i, i = 1, \dots, m^l$  are disjoint, implying that  $\boldsymbol{\xi}_j$  can only belong to one of the partitions: now suppose  $\boldsymbol{\xi}_j \in A_{i'}, i' \in [1, \dots, m^l]$ . Combining all this, we have  $\mathbb{E}_{\pi}[\mathbb{E}_{\mathbf{P}}[h(\mathbf{x}, \boldsymbol{\xi})]] = \mathbb{E}_{\mathbf{P}_0} \frac{\alpha}{\alpha+n} h(\mathbf{x}, \boldsymbol{\xi}) + \frac{1}{\alpha+n} \sum_{j=1}^n h(\mathbf{x}, \boldsymbol{\xi}_j)$ .  $\square$

## EC.2. Proof of consistency.

*Proof of Theorem 1 Proof of (i):* According to Lemma 1, by adding and subtracting  $\frac{1}{n} \sum_{j=1}^n h(\mathbf{x}, \boldsymbol{\xi}_j)$ , we have

$$\begin{aligned} &\mathbb{E}_{\pi}[\mathbb{E}_{\mathbf{P}}[h(\mathbf{x}, \boldsymbol{\xi})]] - \mathbb{E}_{\mathbf{P}^c}[h(\mathbf{x}, \boldsymbol{\xi})] \\ &= \mathbb{E}_{\mathbf{P}_0} \frac{\alpha}{\alpha + n} h(\mathbf{x}, \boldsymbol{\xi}) + \frac{1}{\alpha + n} \sum_{j=1}^n h(\mathbf{x}, \boldsymbol{\xi}_j) - \mathbb{E}_{\mathbf{P}^c}[h(\mathbf{x}, \boldsymbol{\xi})] \\ &= \mathbb{E}_{\mathbf{P}_0} \frac{\alpha}{\alpha + n} h(\mathbf{x}, \boldsymbol{\xi}) + \frac{1}{\alpha + n} \sum_{j=1}^n h(\mathbf{x}, \boldsymbol{\xi}_j) - \frac{1}{n} \sum_{j=1}^n h(\mathbf{x}, \boldsymbol{\xi}_j) + \frac{1}{n} \sum_{j=1}^n (h(\mathbf{x}, \boldsymbol{\xi}_j) - \mathbb{E}_{\mathbf{P}^c}[h(\mathbf{x}, \boldsymbol{\xi})]) \\ &= \frac{\alpha}{\alpha + n} \mathbb{E}_{\mathbf{P}_0} h(\mathbf{x}, \boldsymbol{\xi}) - \frac{\alpha}{(n + \alpha)n} \sum_{j=1}^n h(\mathbf{x}, \boldsymbol{\xi}_j) + \frac{1}{n} \sum_{j=1}^n (h(\mathbf{x}, \boldsymbol{\xi}_j) - \mathbb{E}_{\mathbf{P}^c}[h(\mathbf{x}, \boldsymbol{\xi})]) \end{aligned}$$

The first two terms of the above equation are of order  $o_p(1)$ . We then apply the weak law of large numbers to the last term of the above equation to conclude.

**Proof of (ii):** Since for any  $\boldsymbol{\xi}$ ,  $|h(\mathbf{x}_1, \boldsymbol{\xi}) - h(\mathbf{x}_2, \boldsymbol{\xi})| \leq L_2 \|\mathbf{x}_1 - \mathbf{x}_2\|$  according to Assumption 1, the class of functions  $\mathcal{F} = \{h(\mathbf{x}, \boldsymbol{\xi}) | \mathbf{x} \in \mathbb{R}\}$  is Donsker, from Example 19.6 of Van der Vaart (2000), and thus  $|\mathbb{E}_{\mathcal{P}^c}[h(\mathbf{x}, \boldsymbol{\xi})] - \frac{1}{n} \sum_{j=1}^n h(\mathbf{x}, \boldsymbol{\xi}_j)| \rightarrow_p 0$  uniformly by the property of Donsker class functions (Van der Vaart 2000). Therefore,

$$\sup_{\mathbf{x}} |\mathbb{E}_{\mathcal{P}^c}[h(\mathbf{x}, \boldsymbol{\xi})] - \frac{1}{n} \sum_{j=1}^n h(\mathbf{x}, \boldsymbol{\xi}_j)| \rightarrow_p 0. \quad (\text{EC.2})$$

Equation (EC.2) verify the first condition of Theorem 5.7 of Van der Vaart (2000), now we still need to consider the other condition. In view of the above equation and Lemma 1, we know

$$\begin{aligned} \sup_{\mathbf{x}} |\mathbb{E}_{\pi}[\mathbb{E}_{\mathcal{P}}[h(\mathbf{x}, \boldsymbol{\xi})]] - \frac{1}{n} \sum_{j=1}^n h(\mathbf{x}, \boldsymbol{\xi}_j)| &= \sup_{\mathbf{x}} \left| \frac{\alpha}{\alpha + n} \mathbb{E}_{\mathcal{P}_0} h(\mathbf{x}, \boldsymbol{\xi}) - \frac{\alpha}{(n + \alpha)n} \sum_{j=1}^n h(\mathbf{x}, \boldsymbol{\xi}_j) \right| \\ &\leq \frac{\alpha}{\alpha + n} \sup_{\mathbf{x}} \left( |\mathbb{E}_{\mathcal{P}_0} h(\mathbf{x}, \boldsymbol{\xi})| + \left| \frac{1}{n} \sum_{j=1}^n h(\mathbf{x}, \boldsymbol{\xi}_j) \right| \right) \\ &\leq \frac{2\alpha}{\alpha + n} \sup_{\mathbf{x}, \boldsymbol{\xi}} |h(\mathbf{x}, \boldsymbol{\xi})| = o_p(1). \end{aligned}$$

As  $\mathbf{x}_n = \arg \min_{\mathbf{x}} \mathbb{E}_{\pi}[\mathbb{E}_{\mathcal{P}}[h(\mathbf{x}, \boldsymbol{\xi})]]$  and suppose  $\mathbf{x}' = \arg \min_{\mathbf{x}} \frac{1}{n} \sum_{j=1}^n h(\mathbf{x}, \boldsymbol{\xi}_j)$ , we have

$$\begin{aligned} &\mathbb{E}_{\pi}[\mathbb{E}_{\mathcal{P}}[h(\mathbf{x}_n, \boldsymbol{\xi})]] \leq \mathbb{E}_{\pi}[\mathbb{E}_{\mathcal{P}}[h(\mathbf{x}', \boldsymbol{\xi})]] \\ \Leftrightarrow &\mathbb{E}_{\pi}[\mathbb{E}_{\mathcal{P}}[h(\mathbf{x}_n, \boldsymbol{\xi})]] + \frac{1}{n} \sum_{j=1}^n h(\mathbf{x}_n, \boldsymbol{\xi}_j) - \frac{1}{n} \sum_{j=1}^n h(\mathbf{x}_n, \boldsymbol{\xi}_j) \leq \mathbb{E}_{\pi}[\mathbb{E}_{\mathcal{P}}[h(\mathbf{x}', \boldsymbol{\xi})]] + \frac{1}{n} \sum_{j=1}^n h(\mathbf{x}', \boldsymbol{\xi}_j) - \frac{1}{n} \sum_{j=1}^n h(\mathbf{x}', \boldsymbol{\xi}_j) \end{aligned}$$

Rearranging terms and use absolute value inequality, we have

$$\begin{aligned} \frac{1}{n} \sum_{j=1}^n h(\mathbf{x}_n, \boldsymbol{\xi}_j) &\leq \frac{1}{n} \sum_{j=1}^n h(\mathbf{x}', \boldsymbol{\xi}_j) + \mathbb{E}_{\pi}[\mathbb{E}_{\mathcal{P}}[h(\mathbf{x}', \boldsymbol{\xi})]] - \frac{1}{n} \sum_{j=1}^n h(\mathbf{x}', \boldsymbol{\xi}_j) - \mathbb{E}_{\pi}[\mathbb{E}_{\mathcal{P}}[h(\mathbf{x}_n, \boldsymbol{\xi})]] + \frac{1}{n} \sum_{j=1}^n h(\mathbf{x}_n, \boldsymbol{\xi}_j) \\ &\leq \frac{1}{n} \sum_{j=1}^n h(\mathbf{x}', \boldsymbol{\xi}_j) + \left| \mathbb{E}_{\pi}[\mathbb{E}_{\mathcal{P}}[h(\mathbf{x}', \boldsymbol{\xi})]] - \frac{1}{n} \sum_{j=1}^n h(\mathbf{x}', \boldsymbol{\xi}_j) \right| + \left| \mathbb{E}_{\pi}[\mathbb{E}_{\mathcal{P}}[h(\mathbf{x}_n, \boldsymbol{\xi})]] - \frac{1}{n} \sum_{j=1}^n h(\mathbf{x}_n, \boldsymbol{\xi}_j) \right| \\ &\leq \frac{1}{n} \sum_{j=1}^n h(\mathbf{x}', \boldsymbol{\xi}_j) + o_p(1) \quad \left( \text{as } \sup_{\mathbf{x}} \left| \mathbb{E}_{\pi}[\mathbb{E}_{\mathcal{P}}[h(\mathbf{x}, \boldsymbol{\xi})]] - \frac{1}{n} \sum_{j=1}^n h(\mathbf{x}, \boldsymbol{\xi}_j) \right| = o_p(1) \right) \\ &\leq \frac{1}{n} \sum_{j=1}^n h(\mathbf{x}^*, \boldsymbol{\xi}_j) + o_p(1). \end{aligned} \quad (\text{EC.3})$$

Since all the conditions in Theorem 5.7 of Van der Vaart (2000) are satisfied (Equations (7), (EC.2) and (EC.3)), we conclude the consistency of  $\mathbf{x}_n \rightarrow_p \mathbf{x}^*$ .

**Proof of (iii):** Since for any  $\boldsymbol{\xi}$ ,  $|h(\mathbf{x}_1, \boldsymbol{\xi}) - h(\mathbf{x}_2, \boldsymbol{\xi})| \leq L_2 \|\mathbf{x}_1 - \mathbf{x}_2\|$  from Assumption 1, the class of functions  $\mathcal{F} = \{h(\mathbf{x}, \boldsymbol{\xi}) | \mathbf{x} \in \mathbb{R}\}$  is Donsker, from Example 19.6 of Van der Vaart

(2000). Also since  $\mathbf{x}_n \rightarrow_p \mathbf{x}^*$  from the second part of this theorem, we can use Lemma 19.24 of Van der Vaart (2000) to see

$$\frac{1}{\sqrt{n}} \sum_{j=1}^n h(\mathbf{x}_n, \boldsymbol{\xi}_j) - \frac{1}{\sqrt{n}} \sum_{j=1}^n h(\mathbf{x}^*, \boldsymbol{\xi}_j) = \sqrt{n} (\mathbb{E}_{\mathcal{P}^c}[h(\mathbf{x}_n, \boldsymbol{\xi})] - \mathbb{E}_{\mathcal{P}^c}[h(\mathbf{x}^*, \boldsymbol{\xi})]) + o_p(1)$$

Using the Taylor expansion to deal with the right-hand side of the above equation, and using the fact  $(\mathbb{E}_{\mathcal{P}^c}[h(\mathbf{x}, \boldsymbol{\xi})])'_{\mathbf{x}=\mathbf{x}^*} = 0$ , we obtain

$$\frac{1}{\sqrt{n}} \sum_{j=1}^n h(\mathbf{x}_n, \boldsymbol{\xi}_j) - \frac{1}{\sqrt{n}} \sum_{j=1}^n h(\mathbf{x}^*, \boldsymbol{\xi}_j) = o_p(\sqrt{n}|\mathbf{x}_n - \mathbf{x}^*|). \quad (\text{EC.4})$$

Thus

$$\frac{1}{n} \sum_{j=1}^n h(\mathbf{x}_n, \boldsymbol{\xi}_j) - \frac{1}{n} \sum_{j=1}^n h(\mathbf{x}^*, \boldsymbol{\xi}_j) = o_p(1). \quad (\text{EC.5})$$

By using Lemma 1 and telescoping with  $\frac{1}{n} \sum_{j=1}^n h(\mathbf{x}_n, \boldsymbol{\xi}_j)$ , we can compute that

$$\begin{aligned} & \mathbb{E}_{\boldsymbol{\pi}}[\mathbb{E}_{\mathcal{P}}[h(\mathbf{x}_n, \boldsymbol{\xi})]] - \mathbb{E}_{\mathcal{P}^c}[h(\mathbf{x}^*, \boldsymbol{\xi})] \\ &= \mathbb{E}_{\mathcal{P}_0} \frac{\alpha}{\alpha+n} h(\mathbf{x}_n, \boldsymbol{\xi}) + \frac{1}{\alpha+n} \sum_{j=1}^n h(\mathbf{x}_n, \boldsymbol{\xi}_j) - \mathbb{E}_{\mathcal{P}^c}[h(\mathbf{x}^*, \boldsymbol{\xi})] \\ &= \mathbb{E}_{\mathcal{P}_0} \frac{\alpha}{\alpha+n} h(\mathbf{x}_n, \boldsymbol{\xi}) + \frac{1}{\alpha+n} \sum_{j=1}^n h(\mathbf{x}_n, \boldsymbol{\xi}_j) - \frac{1}{n} \sum_{j=1}^n h(\mathbf{x}_n, \boldsymbol{\xi}_j) + \frac{1}{n} \sum_{j=1}^n h(\mathbf{x}_n, \boldsymbol{\xi}_j) - \mathbb{E}_{\mathcal{P}^c}[h(\mathbf{x}^*, \boldsymbol{\xi})] \\ &= \frac{\alpha}{\alpha+n} \mathbb{E}_{\mathcal{P}_0} h(\mathbf{x}_n, \boldsymbol{\xi}) - \frac{\alpha}{(\alpha+n)n} \sum_{j=1}^n h(\mathbf{x}_n, \boldsymbol{\xi}_j) + \frac{1}{n} \sum_{j=1}^n h(\mathbf{x}_n, \boldsymbol{\xi}_j) - \mathbb{E}_{\mathcal{P}^c}[h(\mathbf{x}^*, \boldsymbol{\xi})] \\ &= o_p(1) + \frac{1}{n} \sum_{j=1}^n h(\mathbf{x}_n, \boldsymbol{\xi}_j) - \mathbb{E}_{\mathcal{P}^c}[h(\mathbf{x}^*, \boldsymbol{\xi})] \\ &= o_p(1) + \left( \frac{1}{n} \sum_{j=1}^n h(\mathbf{x}_n, \boldsymbol{\xi}_j) - \frac{1}{n} \sum_{j=1}^n h(\mathbf{x}^*, \boldsymbol{\xi}_j) \right) + \frac{1}{n} \sum_{j=1}^n (h(\mathbf{x}^*, \boldsymbol{\xi}_j) - \mathbb{E}_{\mathcal{P}^c}[h(\mathbf{x}^*, \boldsymbol{\xi})]) = o_p(1), \end{aligned}$$

where the first equality is due to the definition of  $\mathbb{E}_{\boldsymbol{\pi}}[\mathbb{E}_{\mathcal{P}}[h(\mathbf{x}_n, \boldsymbol{\xi})]]$ , the third equality is by direct computation, and the last equality is due to Equation (EC.5) as well as the weak law of large numbers.  $\square$

### EC.3. Proof of asymptotic normality

*Proof of Theorem 2. Proof of (i):* According to Lemma 1, by adding and subtracting  $\frac{1}{n} \sum_{j=1}^n h(\mathbf{x}, \boldsymbol{\xi}_j)$ , we have

$$\begin{aligned} & \sqrt{n} (\mathbb{E}_\pi[\mathbb{E}_{\mathbf{P}}[h(\mathbf{x}, \boldsymbol{\xi})]] - \mathbb{E}_{\mathbf{P}^c}[h(\mathbf{x}, \boldsymbol{\xi})]) \\ &= \sqrt{n} \left( \mathbb{E}_{\mathbf{P}_0} \frac{\alpha}{\alpha+n} h(\mathbf{x}, \boldsymbol{\xi}) + \frac{1}{\alpha+n} \sum_{j=1}^n h(\mathbf{x}, \boldsymbol{\xi}_j) - \mathbb{E}_{\mathbf{P}^c}[h(\mathbf{x}, \boldsymbol{\xi})] \right) \\ &= \sqrt{n} \left( \mathbb{E}_{\mathbf{P}_0} \frac{\alpha}{\alpha+n} h(\mathbf{x}, \boldsymbol{\xi}) + \frac{1}{\alpha+n} \sum_{j=1}^n h(\mathbf{x}, \boldsymbol{\xi}_j) - \frac{1}{n} \sum_{j=1}^n h(\mathbf{x}, \boldsymbol{\xi}_j) + \frac{1}{n} \sum_{j=1}^n (h(\mathbf{x}, \boldsymbol{\xi}_j) - \mathbb{E}_{\mathbf{P}^c}[h(\mathbf{x}, \boldsymbol{\xi})]) \right) \\ &= \frac{\sqrt{n}\alpha}{\alpha+n} \mathbb{E}_{\mathbf{P}_0} h(\mathbf{x}, \boldsymbol{\xi}) - \frac{\alpha}{(n+\alpha)\sqrt{n}} \sum_{j=1}^n h(\mathbf{x}, \boldsymbol{\xi}_j) + \frac{1}{\sqrt{n}} \sum_{j=1}^n (h(\mathbf{x}, \boldsymbol{\xi}_j) - \mathbb{E}_{\mathbf{P}^c}[h(\mathbf{x}, \boldsymbol{\xi})]) \end{aligned}$$

The first two terms of the above equation are of order  $o_p(1)$ , which do not affect the asymptotic distribution of  $\sqrt{n} (\mathbb{E}_\pi[\mathbb{E}_{\mathbf{P}}[h(\mathbf{x}, \boldsymbol{\xi})]] - \mathbb{E}_{\mathbf{P}^c}[h(\mathbf{x}, \boldsymbol{\xi})])$ . We then apply the central limit theorem to the last term of the above equation to conclude.

**Proof of (ii):** Since  $\mathbf{x}_n$  minimize  $\mathbb{E}_\pi[\mathbb{E}_{\mathbf{P}}[h(\mathbf{x}, \boldsymbol{\xi})]]$ ,

$$\mathbb{E}_{\mathbf{P}_0} \frac{\alpha}{\alpha+n} \partial_{\mathbf{x}} h(\mathbf{x}_n, \boldsymbol{\xi}) + \frac{1}{\alpha+n} \sum_{j=1}^n \partial_{\mathbf{x}} h(\mathbf{x}_n, \boldsymbol{\xi}_j) = 0.$$

Using the above equation and the fact  $\frac{1}{n} \sum_{j=1}^n \partial_{\mathbf{x}} h(\mathbf{x}_n, \boldsymbol{\xi}_j) = \frac{1}{\alpha+n} \sum_{j=1}^n \partial_{\mathbf{x}} h(\mathbf{x}_n, \boldsymbol{\xi}_j) + \frac{\alpha}{n(n+\alpha)} \sum_{j=1}^n \partial_{\mathbf{x}} h(\mathbf{x}_n, \boldsymbol{\xi}_j)$ , the following equality is immediate:

$$\begin{aligned} \frac{1}{n} \sum_{j=1}^n \partial_{\mathbf{x}} h(\mathbf{x}_n, \boldsymbol{\xi}_j) &= \mathbb{E}_{\mathbf{P}_0} \frac{\alpha}{n+\alpha} \partial_{\mathbf{x}} h(\mathbf{x}_n, \boldsymbol{\xi}) + \frac{1}{\alpha+n} \sum_{j=1}^n \partial_{\mathbf{x}} h(\mathbf{x}_n, \boldsymbol{\xi}_j) - \\ &\quad \left( \mathbb{E}_{\mathbf{P}_0} \frac{\alpha}{n+\alpha} \partial_{\mathbf{x}} h(\mathbf{x}_n, \boldsymbol{\xi}) - \frac{\alpha}{n(n+\alpha)} \sum_{j=1}^n \partial_{\mathbf{x}} h(\mathbf{x}_n, \boldsymbol{\xi}_j) \right) = o_p\left(\frac{1}{\sqrt{n}}\right) \end{aligned}$$

The last equality holds due to the fact that  $\mathbb{E}_{\mathbf{P}_0} \frac{\alpha}{n+\alpha} \partial_{\mathbf{x}} h(\mathbf{x}_n, \boldsymbol{\xi}) - \frac{\alpha}{n(n+\alpha)} \sum_{j=1}^n \partial_{\mathbf{x}} h(\mathbf{x}_n, \boldsymbol{\xi}_j) = O_p\left(\frac{1}{n}\right) = o_p\left(\frac{1}{\sqrt{n}}\right)$ . Since  $\partial_{\mathbf{x}} h(\mathbf{x}, \boldsymbol{\xi})$  is Lipschitz in  $\mathbf{x}$  (Assumption 1(i)),  $\mathbf{x}_n \rightarrow_p \mathbf{x}^*$ , and  $\frac{1}{n} \sum_{j=1}^n \partial_{\mathbf{x}} h(\mathbf{x}_n, \boldsymbol{\xi}_j) = o_p\left(\frac{1}{\sqrt{n}}\right)$ , we have verified the conditions in Theorem 5.21 of Van der Vaart (2000), and so  $\sqrt{n}(\mathbf{x}_n - \mathbf{x}^*)$  is asymptotically normal distributed with mean zero and variance  $\sigma_x^2 = \mathbb{E}_{\mathbf{P}^c} \left( \frac{\partial h(\mathbf{x}^*, \boldsymbol{\xi})}{\partial \mathbf{x}} \right)^2 / \left( \frac{\partial^2 \mathbb{E}_{\mathbf{P}^c}[h(\mathbf{x}^*, \boldsymbol{\xi})]}{\partial \mathbf{x}^2} \right)^2 = \mathbb{E}_{\mathbf{P}^c} \left( \frac{\partial h(\mathbf{x}^*, \boldsymbol{\xi})}{\partial \mathbf{x}} \right)^2 / (f''(\mathbf{x}^*))^2$  from Theorem 5.21 of Van der Vaart (2000).

**Proof of (iii):** As  $\sqrt{n}(\mathbf{x}_n - \mathbf{x}^*)$  is asymptotically normally distributed from the previous part of this theorem, we know  $\sqrt{n}|\mathbf{x}_n - \mathbf{x}^*| = O_p(1)$ . Then according to Equation (EC.4), we have

$$\frac{1}{\sqrt{n}} \sum_{j=1}^n h(\mathbf{x}_n, \boldsymbol{\xi}_j) - \frac{1}{\sqrt{n}} \sum_{j=1}^n h(\mathbf{x}^*, \boldsymbol{\xi}_j) = o_p(\sqrt{n}|\mathbf{x}_n - \mathbf{x}^*|) = o_p(1).$$

By using Lemma 1 and telescoping with  $\frac{1}{n} \sum_{j=1}^n h(\mathbf{x}_n, \boldsymbol{\xi}_j)$ , we have

$$\begin{aligned} & \sqrt{n} (\mathbb{E}_\pi[\mathbb{E}_P[h(\mathbf{x}_n, \boldsymbol{\xi})]] - \mathbb{E}_{P^c}[h(\mathbf{x}^*, \boldsymbol{\xi})]) \\ &= \sqrt{n} \left( \mathbb{E}_{P_0} \frac{\alpha}{\alpha+n} h(\mathbf{x}_n, \boldsymbol{\xi}) + \frac{1}{\alpha+n} \sum_{j=1}^n h(\mathbf{x}_n, \boldsymbol{\xi}_j) - \mathbb{E}_{P^c}[h(\mathbf{x}^*, \boldsymbol{\xi})] \right) \\ &= \sqrt{n} \left( \mathbb{E}_{P_0} \frac{\alpha}{\alpha+n} h(\mathbf{x}_n, \boldsymbol{\xi}) + \frac{1}{\alpha+n} \sum_{j=1}^n h(\mathbf{x}_n, \boldsymbol{\xi}_j) - \frac{1}{n} \sum_{j=1}^n h(\mathbf{x}_n, \boldsymbol{\xi}_j) + \frac{1}{n} \sum_{j=1}^n h(\mathbf{x}_n, \boldsymbol{\xi}_j) - \mathbb{E}_{P^c}[h(\mathbf{x}^*, \boldsymbol{\xi})] \right) \\ &= \mathbb{E}_{P_0} \frac{\sqrt{n}\alpha}{\alpha+n} h(\mathbf{x}_n, \boldsymbol{\xi}) - \frac{\alpha}{(\alpha+n)\sqrt{n}} \sum_{j=1}^n h(\mathbf{x}_n, \boldsymbol{\xi}_j) + \frac{1}{\sqrt{n}} \sum_{j=1}^n h(\mathbf{x}_n, \boldsymbol{\xi}_j) - \sqrt{n} \mathbb{E}_{P^c}[h(\mathbf{x}^*, \boldsymbol{\xi})] \\ &= \mathbb{E}_{P_0} \frac{\sqrt{n}\alpha}{\alpha+n} h(\mathbf{x}_n, \boldsymbol{\xi}) - \frac{\alpha}{(\alpha+n)\sqrt{n}} \sum_{j=1}^n h(\mathbf{x}_n, \boldsymbol{\xi}_j) + \frac{1}{\sqrt{n}} \sum_{j=1}^n h(\mathbf{x}_n, \boldsymbol{\xi}_j) - \frac{1}{\sqrt{n}} \sum_{j=1}^n h(\mathbf{x}^*, \boldsymbol{\xi}_j) \\ & \quad + \frac{1}{\sqrt{n}} \sum_{j=1}^n h(\mathbf{x}^*, \boldsymbol{\xi}_j) - \sqrt{n} \mathbb{E}_{P^c}[h(\mathbf{x}^*, \boldsymbol{\xi})] \end{aligned}$$

The sum of the first two terms of the last equality is of order  $o_p(1)$  since  $h$  is bounded. We can then use the fact that  $\frac{1}{\sqrt{n}} \sum_{j=1}^n h(\mathbf{x}_n, \boldsymbol{\xi}_j) - \frac{1}{\sqrt{n}} \sum_{j=1}^n h(\mathbf{x}^*, \boldsymbol{\xi}_j) = o_p(1)$  to reformulate the last equality of the above equation as

$$\sqrt{n} (\mathbb{E}_\pi[\mathbb{E}_P[h(\mathbf{x}_n, \boldsymbol{\xi})]] - \mathbb{E}_{P^c}[h(\mathbf{x}^*, \boldsymbol{\xi})]) = o_p(1) + \frac{1}{\sqrt{n}} \sum_{j=1}^n (h(\mathbf{x}^*, \boldsymbol{\xi}_j) - \mathbb{E}_{P^c}[h(\mathbf{x}^*, \boldsymbol{\xi})])$$

According to the central limit theorem,  $\frac{1}{\sqrt{n}} \sum_{j=1}^n (h(\mathbf{x}^*, \boldsymbol{\xi}_j) - \mathbb{E}_{P^c}[h(\mathbf{x}^*, \boldsymbol{\xi})])$  is asymptotically normally distributed with mean zero and variance  $\text{Var}(h(\mathbf{x}^*, \boldsymbol{\xi}))$ .  $\square$

#### EC.4. Proof of the convergence of algorithm

*Proof of Theorem 3.* The proof of this theorem is decomposed into two main steps. In the first step, we aim to show that:

$$|\mu_s(\mathbf{x}) - g(\mathbf{x})| \rightarrow_p 0 \tag{EC.6}$$

uniformly for all  $\mathbf{x}$ . In the second step, we are going to show that the points we visit in our algorithm are dense. These two results then naturally imply the convergence of our algorithm. First look at the first step, since

$$|\mu_s(\mathbf{x}) - g(\mathbf{x})| \leq |\mu_s(\mathbf{x}) - \mathbb{E}_{P \sim \pi}[F_s(\mathbf{x}, \mathbf{P})]| + |\mathbb{E}_{P \sim \pi}[F_s(\mathbf{x}, \mathbf{P})] - g(\mathbf{x})|,$$

from the triangle inequality,

$$\begin{aligned} \mathbb{P}\{|\mu_s(\mathbf{x}) - g(\mathbf{x})| \geq 2\epsilon\} &\leq \mathbb{P}\{|\mu_s(\mathbf{x}) - \mathbb{E}_{\mathbf{P} \sim \pi} F_s(\mathbf{x}, \mathbf{P})| + |\mathbb{E}_{\mathbf{P} \sim \pi} F_s(\mathbf{x}, \mathbf{P}) - g(\mathbf{x})| \geq 2\epsilon\} \\ &\leq \mathbb{P}\{|\mu_s(\mathbf{x}) - \mathbb{E}_{\mathbf{P} \sim \pi} F_s(\mathbf{x}, \mathbf{P})| \geq \epsilon\} + \mathbb{P}\{|\mathbb{E}_{\mathbf{P} \sim \pi} F_s(\mathbf{x}, \mathbf{P}) - g(\mathbf{x})| \geq \epsilon\}. \end{aligned}$$

Thus, to establish Equation (EC.6), it suffices to establish

$$\mu_s(\mathbf{x}) - \mathbb{E}_{\mathbf{P} \sim \pi} F_s(\mathbf{x}, \mathbf{P}) \rightarrow_p 0, \quad \text{and} \quad \mathbb{E}_{\mathbf{P} \sim \pi} F_s(\mathbf{x}, \mathbf{P}) - g(\mathbf{x}) \rightarrow_p 0$$

Now, suppose we could directly observe  $f(\mathbf{x}, \mathbf{P})$  and construct a deterministic GP model with conditional mean  $\tilde{m}_s(\mathbf{x}, \mathbf{P})$  and conditional variance  $\tilde{k}_s((\mathbf{x}, \mathbf{P}), (\mathbf{x}, \mathbf{P}))$ . We have

$$|F_s(\mathbf{x}, \mathbf{P}) - f(\mathbf{x}, \mathbf{P})| \leq \underbrace{|F_s(\mathbf{x}, \mathbf{P}) - m_s(\mathbf{x}, \mathbf{P})|}_A + \underbrace{|m_s(\mathbf{x}, \mathbf{P}) - \tilde{m}_s(\mathbf{x}, \mathbf{P})|}_B + \underbrace{|\tilde{m}_s(\mathbf{x}, \mathbf{P}) - f(\mathbf{x}, \mathbf{P})|}_C$$

Direct calculations show that

$$\tilde{m}_s(\mathbf{x}, \mathbf{P}) - m_s(\mathbf{x}, \mathbf{P}) \rightarrow_p 0 \quad \text{and} \quad \tilde{k}_s((\mathbf{x}, \mathbf{P}), (\mathbf{x}, \mathbf{P})) - k_s((\mathbf{x}, \mathbf{P}), (\mathbf{x}, \mathbf{P})) \rightarrow_p 0$$

uniformly in  $\mathbf{x}$  as the number of replications  $r$  tends to infinity (Lemma 5 of [Pedrielli et al. \(2020\)](#)). And so part  $B$  tends to zero uniformly. According to Propositions 3.3, 3.4 and 3.5 of [Stuart and Teckentrup \(2018\)](#), we have  $\tilde{m}_s(\mathbf{x}, \mathbf{P}) - f(\mathbf{x}, \mathbf{P}) \rightarrow_p 0$ , and  $k_s((\mathbf{x}, \mathbf{P}), (\mathbf{x}, \mathbf{P})) \rightarrow_p 0$ , uniformly for all  $(\mathbf{x}, \mathbf{P})$ . And so part  $C$  tends to zero as  $s$  tends to infinity. For part  $A$ , the expectation of  $F_s(\mathbf{x}, \mathbf{P})$  is  $m_s(\mathbf{x}, \mathbf{P})$  and the marginal variance  $k_s$  tends to zero uniformly. Thus part  $A$  also converges to zero in probability uniformly for  $(\mathbf{x}, \mathbf{P})$  from Chebyshev's Inequality:

$$\mathbb{P}(|F_s(\mathbf{x}, \mathbf{P}) - m_s(\mathbf{x}, \mathbf{P})| \geq \epsilon) \leq \frac{k_s((\mathbf{x}, \mathbf{P}), (\mathbf{x}, \mathbf{P}))}{\epsilon^2}.$$

Combining all that we know,

$$|F_s(\mathbf{x}, \mathbf{P}) - f(\mathbf{x}, \mathbf{P})| \rightarrow_p 0$$

uniformly for all  $(\mathbf{x}, \mathbf{P})$ . And so

$$\begin{aligned} \sup_{\mathbf{x}} |\mathbb{E}_{\mathbf{P} \sim \pi} F_s(\mathbf{x}, \mathbf{P}) - g(\mathbf{x})| &= \sup_{\mathbf{x}} |\mathbb{E}_{\mathbf{P} \sim \pi} (F_s(\mathbf{x}, \mathbf{P}) - f(\mathbf{x}, \mathbf{P}))| \\ &\leq \sup_{\mathbf{x}, \mathbf{P}} |(F_s(\mathbf{x}, \mathbf{P}) - f(\mathbf{x}, \mathbf{P}))| \rightarrow_p 0, \end{aligned} \tag{EC.7}$$



i.e.,  $\mathbb{E}_{\mathbf{P} \sim \pi} F_s(\mathbf{x}, \mathbf{P}) - g(\mathbf{x}) \rightarrow_p 0$  uniformly in  $\mathbf{x}$ . In addition,

$$\begin{aligned} |\mu_s(\mathbf{x}) - \mathbb{E}_{\mathbf{P} \sim \pi} F_s(\mathbf{x}, \mathbf{P})| &= |\mu_s(\mathbf{x}) - \mathbb{E}_{\mathbf{P} \sim \pi} m_s(\mathbf{x}, \mathbf{P}) + \mathbb{E}_{\mathbf{P} \sim \pi} m_s(\mathbf{x}, \mathbf{P}) - \mathbb{E}_{\mathbf{P} \sim \pi} F_s(\mathbf{x}, \mathbf{P})| \\ &\leq |\mu_s(\mathbf{x}) - \mathbb{E}_{\mathbf{P} \sim \pi} m_s(\mathbf{x}, \mathbf{P})| + |\mathbb{E}_{\mathbf{P} \sim \pi} m_s(\mathbf{x}, \mathbf{P}) - \mathbb{E}_{\mathbf{P} \sim \pi} F_s(\mathbf{x}, \mathbf{P})| \end{aligned}$$

Recall

$$\mu_s(\mathbf{x}) = \frac{1}{N_{mc}} \sum_{i=1}^{N_{mc}} m_s(\mathbf{x}, \mathbf{P}_i).$$

By definition,  $m_s(\mathbf{x}, \mathbf{P})$  is uniformly bounded for all  $\mathbf{x}$  and  $\mathbf{P}$  and so Chebyshev's Inequality implies

$$\mathbb{P}\{|\mu_s(\mathbf{x}) - \mathbb{E}_{\mathbf{P} \sim \pi} m_s(\mathbf{x}, \mathbf{P})| \geq \epsilon\} \leq \frac{\mathbb{E}_{\mathbf{P} \sim \pi} m_s^2(\mathbf{x}, \mathbf{P}) - (\mathbb{E}_{\mathbf{P} \sim \pi} m_s(\mathbf{x}, \mathbf{P}))^2}{\epsilon^2 N_{mc}}.$$

And so  $\mu_s(\mathbf{x}) - \mathbb{E}_{\mathbf{P} \sim \pi} m_s(\mathbf{x}, \mathbf{P}) \rightarrow_p 0$  uniformly in  $\mathbf{x}$  as  $N_{mc} \rightarrow \infty$ . On the other hand,

$$\sup_{\mathbf{x}} |\mathbb{E}_{\mathbf{P} \sim \pi} m_s(\mathbf{x}, \mathbf{P}) - \mathbb{E}_{\mathbf{P} \sim \pi} F_s(\mathbf{x}, \mathbf{P})| \leq \sup_{\mathbf{x}, \mathbf{P}} |m_s(\mathbf{x}, \mathbf{P}) - F_s(\mathbf{x}, \mathbf{P})|$$

The right-hand side converges to zero in probability uniformly and so  $\mathbb{E}_{\mathbf{P} \sim \pi} m_s(\mathbf{x}, \mathbf{P}) - \mathbb{E}_{\mathbf{P} \sim \pi} F_s(\mathbf{x}, \mathbf{P}) \rightarrow_p 0$ . So  $\mu_s(\mathbf{x}) - \mathbb{E}_{\mathbf{P} \sim \pi} F_s(\mathbf{x}, \mathbf{P}) \rightarrow_p 0$  uniformly in  $\mathbf{x}$ . In view of Equation (EC.7), we have completed the proof of  $|\mu_s(\mathbf{x}) - g(\mathbf{x})| \rightarrow_p 0$ .

We then move on to the second step of the proof, i.e., to establish the density of the points we visit. The proof follows similar procedures as Lemma 1 of [Locatelli \(1997\)](#), albeit in a multiple dimensional setting as in [Wang et al. \(2019b\)](#). We consider the following stopping rule in the algorithm: we continue the algorithm while the maximum expected improvement  $\mathbb{E}I_T(\mathbf{x}_{s+1}, \mathbf{P}_{s+1})$  is above some pre-determined constant  $c$  (which is allowed to be arbitrary small in this setting). Recall the definition of  $\mathbb{E}I_T(\mathbf{x}_{s+1}, \mathbf{P}_{s+1})$ :

$$\mathbb{E}I_T(\mathbf{x}_{s+1}, \mathbf{P}_{s+1}) = \Delta \Phi\left(\frac{\Delta}{\sigma'_s(\mathbf{x}_{s+1})}\right) + \sigma'_s(\mathbf{x}_{s+1}) \phi\left(\frac{\Delta}{\sigma'_s(\mathbf{x}_{s+1})}\right)$$

Where  $\Delta = T - \mu_s(\mathbf{x}_{s+1})$  and  $T = \min\{\mu(\mathbf{x}_1), \dots, \mu(\mathbf{x}_s)\}$ . We now claim that  $\mathbf{x}_{s+1}$  cannot be too close to any of the current evaluated points. Otherwise, suppose  $\mu_s(\mathbf{x}_i) = T$  for  $i \in U \subseteq \{1, 2, 3, \dots, s\}$ . If  $\mathbf{x}_{s+1}$  tends to some point in  $U$ , then  $\Delta \rightarrow 0$  and  $\sigma'_s(\mathbf{x}_{s+1}) \rightarrow 0$ . By definition we know  $\mathbb{E}I_T(\mathbf{x}_{s+1}, \mathbf{P}_{s+1}) \rightarrow 0$ . On the other hand, if  $\mathbf{x}_{s+1}$  tends to some point  $x_k$  in  $\{1, 2, 3, \dots, s\}/U$ , then  $\Delta \rightarrow T - \mu_s(\mathbf{x}_k) < 0$  and  $\sigma'_s(\mathbf{x}_{s+1}) \rightarrow 0$ . As a result,  $\Delta \Phi\left(\frac{\Delta}{\sigma'_s(\mathbf{x}_{s+1})}\right) \rightarrow (T - \mu_s(\mathbf{x}_k))\Phi(-\infty) = 0$  and so  $\mathbb{E}I_T(\mathbf{x}_{s+1}, \mathbf{P}_{s+1}) \rightarrow 0$ . Thus, according to our stopping rule that the algorithm will stop when  $\mathbb{E}I_T < c$  for any candidate point for

some value of  $c$ , we cannot select a  $\mathbf{x}_{s+1}$  that is too close to any of the visited points. From Theorem 1 of Locatelli (1997), the algorithm will terminate within a finite number of steps. Lemma 1 of Locatelli (1997) implies that if we decrease the the value of  $c$  to zero, the points we visited will be dense.

As the evaluation points we visited are dense, there will exist a subsequence  $\mathbf{x}_{s_k}$ ,  $k = 1, 2, \dots$  such that  $\mathbf{x}_{s_k} \rightarrow_p \mathbf{x}_n$ . Denote the estimated estimator at  $s_k$ -th iteration by  $\hat{\mathbf{x}}_{s_k}^*$ . For  $s_i < N < s_j$ , as  $s_i$  and  $N$  go to infinity, we have

$$\mu_N(\hat{\mathbf{x}}_N^*) \leq \mu_N(\hat{\mathbf{x}}_{s_i}^*) \leq g(\hat{\mathbf{x}}_{s_i}^*) + o_p(1) = g(\mathbf{x}_n) + (g(\hat{\mathbf{x}}_{s_i}^*) - g(\mathbf{x}_n)) + o_p(1) = g(\mathbf{x}_n) + o_p(1) \quad (\text{EC.8})$$

The first inequality  $\mu_N(\hat{\mathbf{x}}_N^*) \leq \mu_N(\hat{\mathbf{x}}_{s_i}^*)$  is due to the definition of  $\hat{\mathbf{x}}_N^*$ . The second inequality is due to the uniform convergence of  $|\mu_s(\mathbf{x}) - g(\mathbf{x})| \rightarrow_p 0$ . The last equality is due to the continuous mapping theorem. With (EC.8), we have

$$g(\hat{\mathbf{x}}_N^*) \leq \mu_N(\hat{\mathbf{x}}_N^*) + o_p(1) \leq g(\mathbf{x}_n) + o_p(1). \quad \square$$

*Proof of Corollary 1* Now since  $\mathbf{x}_n$  is unique, we can use the fact that  $g$  is continuous at  $\mathbf{x}_n$  to see

$$\inf_{|\mathbf{x} - \mathbf{x}_n| > \epsilon} g(\mathbf{x}) > g(\mathbf{x}_n)$$

for all  $\epsilon > 0$ . And so for any  $\epsilon > 0$ , there exist a  $\delta > 0$  such that

$$g(\mathbf{x}) - g(\mathbf{x}_n) > \delta, \quad \text{for all } |\mathbf{x} - \mathbf{x}_n| > \epsilon.$$

And so

$$\mathbb{P}(|\hat{\mathbf{x}}_N^* - \mathbf{x}_n| > \epsilon) \leq \mathbb{P}(g(\hat{\mathbf{x}}_N^*) - g(\mathbf{x}_n) > \delta) \rightarrow 0, \quad \text{as } N \rightarrow \infty.$$

The last step holds due to Theorem 3.  $\square$

*Proof of Corollary 2* In view of part (ii) of Theorem 1, we can first choose  $n_0$  such that, for any  $n' > n_0$ ,

$$P(|\mathbf{x}_{n'} - \mathbf{x}^*| \geq \frac{\epsilon}{2}) < \frac{\epsilon}{2}. \quad (\text{EC.9})$$

Now for any selected  $n'$ , we use Corollary 1 to see that there exist  $N'$  such that, for any  $N \geq N'$ ,

$$P(|\hat{\mathbf{x}}_N^* - \mathbf{x}_{n'}| \geq \frac{\epsilon}{2}) < \frac{\epsilon}{2}. \quad (\text{EC.10})$$

Combining (EC.9)-(EC.10), the following inequality is immediate:

$$\mathbb{P}(|\hat{\mathbf{x}}_N^* - \mathbf{x}^*| \geq \epsilon) \leq P(|\hat{\mathbf{x}}_N^* - \mathbf{x}_{n'}| \geq \frac{\epsilon}{2}) + P(|\mathbf{x}_{n'} - \mathbf{x}^*| \geq \frac{\epsilon}{2}) < \epsilon.$$

For the convergence of the optimal value, we first use part (iii) of Theorem 1 to see that there exist  $n_0$  such that, for any  $n' > n_0$ ,

$$P(|g(\mathbf{x}_{n'}) - f(\mathbf{x}^*, \mathbf{P}^c)| > \frac{\epsilon}{2}) < \frac{\epsilon}{2}. \quad (\text{EC.11})$$

Then for any fixed  $n'$ , we use Theorem 3 to see that there exists  $N'$  such that, for any  $N > N'$ ,

$$P(|g(\hat{\mathbf{x}}_N^*) - g(\mathbf{x}_{n'})| > \frac{\epsilon}{2}) < \frac{\epsilon}{2}. \quad (\text{EC.12})$$

Combining (EC.11)-(EC.12), the following inequality is immediate:

$$P(|g(\hat{\mathbf{x}}_N^*) - f(\mathbf{x}^*, \mathbf{P}^c)| \geq \epsilon) < P(|g(\hat{\mathbf{x}}_N^*) - g(\mathbf{x}_{n'})| > \frac{\epsilon}{2}) + P(|g(\mathbf{x}_{n'}) - f(\mathbf{x}^*, \mathbf{P}^c)| > \frac{\epsilon}{2}) < \epsilon. \quad \square$$